The metal Abundance Properties of cool-core Clusters

Sabrina De Grandi (INAF-OA Brera Milan, Italy)

Collaborators:

S. Molendi (INAF-IASF Milan), J. Santos (ESAC Madrid) , M. Nonino (INAF-OA Trieste), P. Tozzi (INAF-OA Arcetri), A. Fritz (INAF-IASF Milan), M. Rossetti (Milan Univ.)

Motivations

We are interested in the study of

- evolutionary processes
- enrichment mechanisms

at work in the central region of relaxed clusters of galaxies, which are intrinsically connected with the presence of the Brightest Cluster Galaxy (BCG)

First Part:

- How well do we measure abundances in cluster cores with XMM?
- Focus on the abundance measurements in the centers of local CC clusters

Second Part:

- Properties of the distant cluster WARP J1415.1+3612 at z=1.03

Deriving chemical abundances from the X-ray cluster spectrum of the ICM

Simulated ICM spectrum

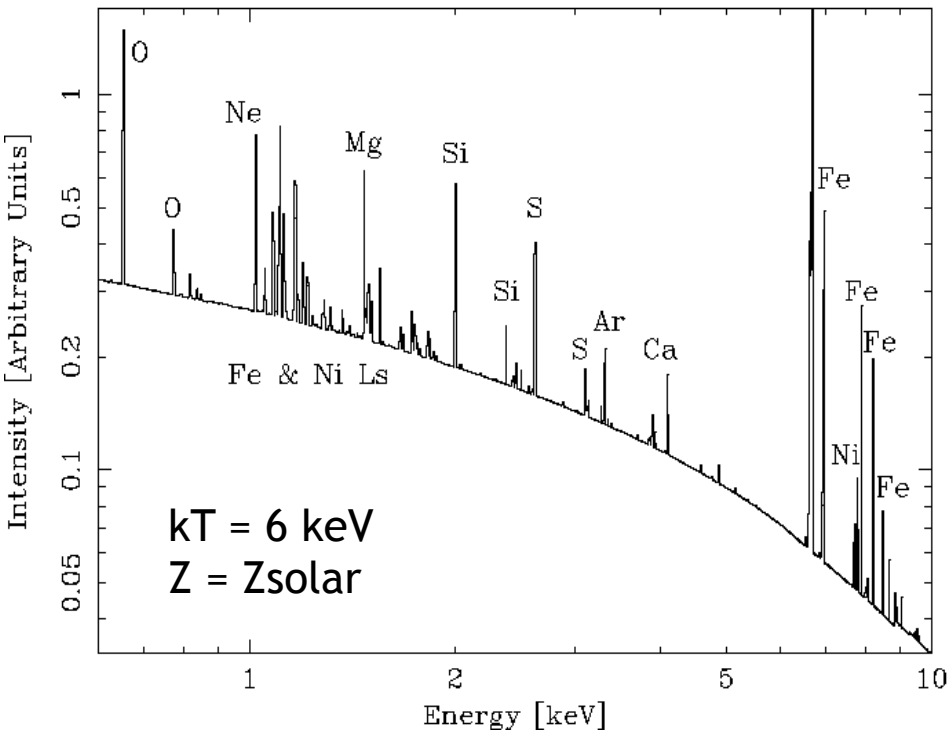

Spectral shape → T_g

$$\varepsilon_\nu \propto n_g^2 \cdot T_g^{-1/2} \cdot e^{-\frac{h\nu}{KT_g}}$$

Normalization → n_g

$$L \propto n_e^2 T_g^{1/2} V$$

Line Equivalent Width → Z

$$EW \equiv \int \frac{I_{line}}{I_{count}} d\upsilon \propto \int \frac{\varepsilon_{line}}{\varepsilon_{ff}} \propto \frac{n_Z}{n_p}$$

Deriving chemical abundances from the X-ray cluster spectrum of the ICM

While in principle abundance measurement is straightforward, in practice various sources of uncertainties are present:

1. The accuracy of the atomic physics
2. The moderate spectral resolution of the current imaging instruments which often results in line blending
3. The presence of temperature gradients in the ICM, especially in cluster cores, that needs specific spectral modeling.

With Chandra/XMM statistical errors have greatly decreased, however little attention was devoted to systematic errors which, under some circumstances, are likely to play an important role.

Our goal is to provide "robust estimates" of chemical elements (Si, Fe, Ni) in the cores of nearby and bright cool-core clusters, i.e. we will include in the error budget a careful evaluation of systematic uncertainties (XMM) (I will only summarize the results)

The Cluster Sample

- **Starting sample is the flux-limited B55 (Edge et al. 1990):**
  - 26 Cool-Core clusters with XMM/EPIC archival data
  - Core regions only: $r<0.5\ r_{cool}$ (r_{cool} from Peres+98)
  - Measure of Si, Fe, Ni (1.8-10. keV E band)

- **Why global Abundance in the CC?**

- In CC there are very intense SB peaks
- central regions provide the maximum photon statistics
- this allows us to explore systematic errors on derived elements in great details
- $0.5r_{cool}$ is a good sampling of the core region and is within EPIC fov

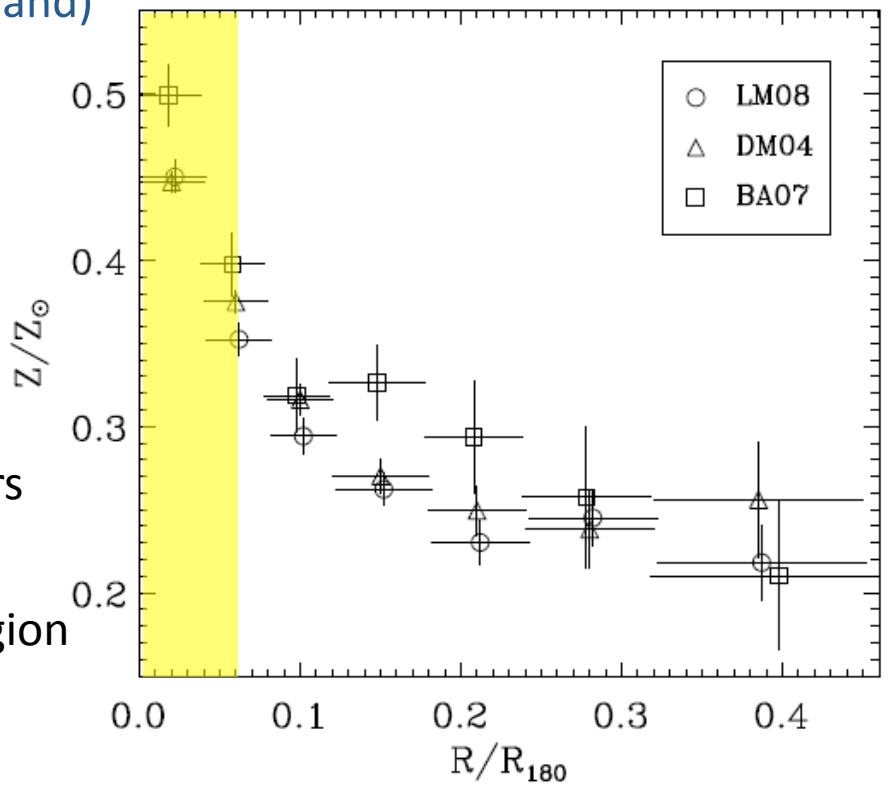

Study of Systematics: Fe-biases when using 1T model instead of multi-T model

- Several works (Rasia et al.+08, Simionescu+09, Gastaldello+10) found evidences of an "Inverse" Fe-bias (i.e. Z_{Fe} too high) when multi-T ICM, with mean kT~2-3 keV, was fitted with single T models
- This bias could affect studies of the global (or central) Z_{Fe} vs. kT relation from SUZAKU/ ASCA/XMM measurements (e.g. Baumgartner+05) or Z_{Fe} measurements in distant cool core clusters (e.g. Balestra+08).
- We use our sample (with strong kT grad!) to study Fe-biases in the kT range ~2-6 keV

Fe-Bias:
kT < 2 keV
with 1T mod
(Fe too low)

Buote+00
(galaxygroups)

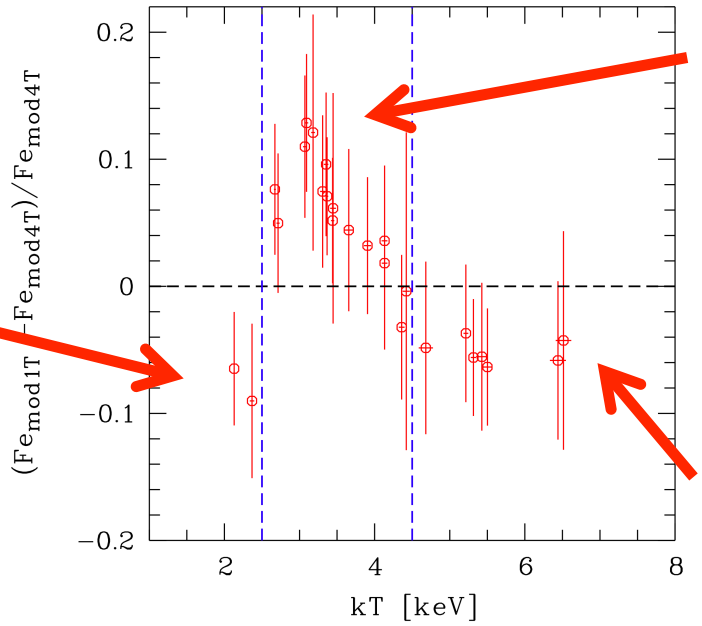

"Inverse" Fe-Bias
2.5 < kT < 4.5 keV
with 1T mod
(Fe too high)

Small Fe-bias
at kT > 5 keV

Although Fe-biases are present at any kT>2keV, they are modest effects, i.e. < 10%

Study of Systematics

- **Fe-biases arising when multi-T ICM is modeled as 1T plasma:** evidence for Fe-biases as a function of plasma mean kT, in the ~2 – 6 keV range, < 5% - 10%
- **Spectral model:** different multi-T models (2T, 4T, mphase,..) give systematic errors on abundance measurements < 2% - 3%
- **EPIC (M1,M2,pn) cross-calibration:** 3% systematic differences for Fe and Si btw the 3 detectors (Ni is dominated by statistical errors)
- **Plasma code (mekal vs apec):** measure EW from a line → Z_i

Study of Systematics

- **Fe-biases arising when multi-T ICM is modeled as 1T plasma:** evidence for Fe-biases as a function of plasma mean kT, in the ~2 – 6 keV range, < 5% - 10%
- **Spectral model:** different multi-T models (2T, 4T, mphase,..) give systematic errors on abundance measurements < 2% - 3%
- **EPIC (M1,M2,pn) cross-calibration:** 3% systematic differences for Fe and Si btw the 3 detectors (Ni is dominated by statistical errors)
- **Plasma code (mekal vs apec)**: measure EW from a line → Z_i
  This is the largest source of systematic errors, significant differences for Fe (4%) and Si/Fe (6%), dominant source of indetermination for Si (10%), Ni (15%), Ni/Fe (20%)

- **Conclusion: systematic sources of errors in Fe and Si/Fe measurements with XMM are well known and are ~ 5% and we are able to handle them.**

Distribution of central abundances

De Grandi et al. 09

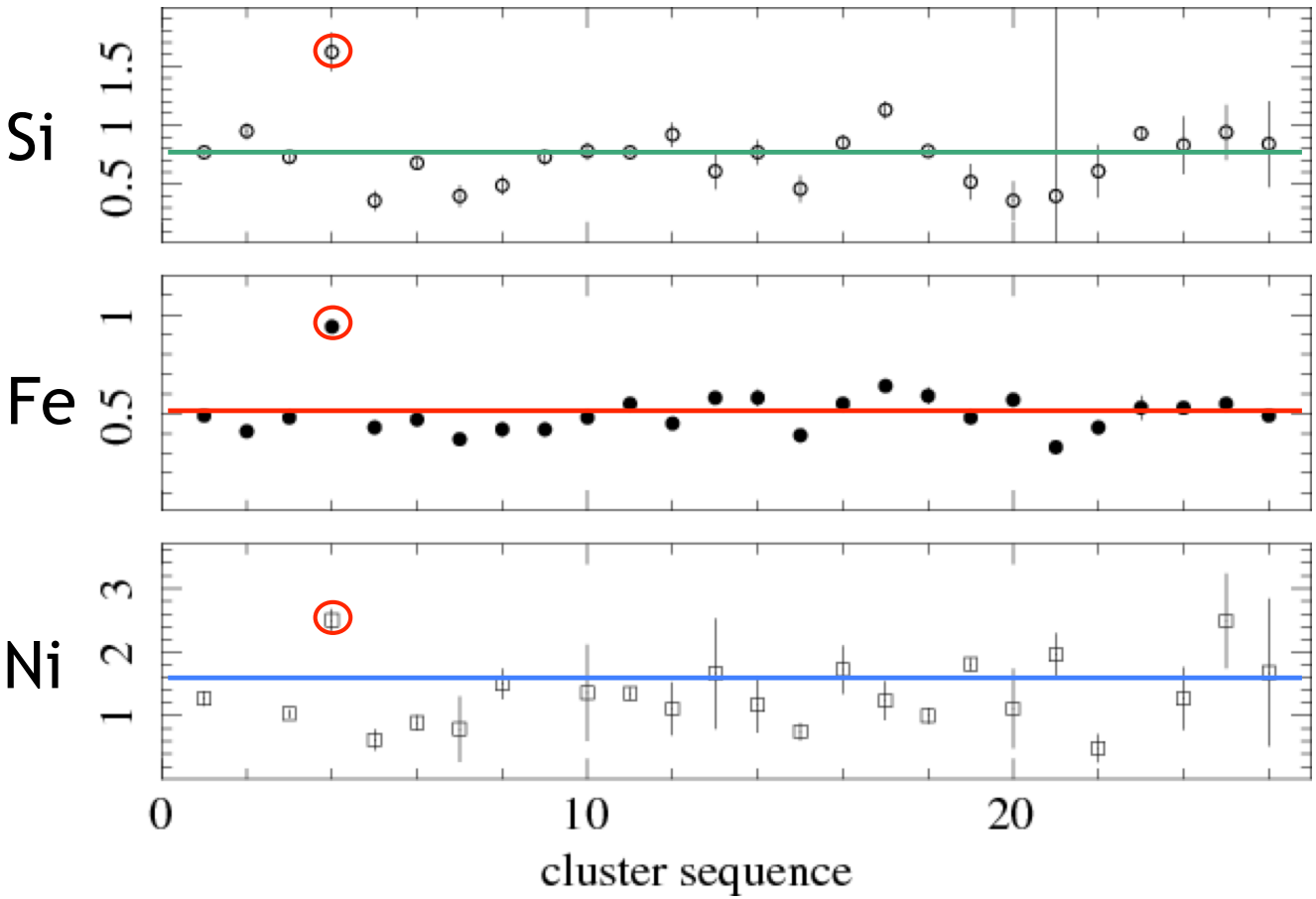

0.75 ± 0.03

$\sigma_{Si} \sim 30\%$

0.51 ± 0.02

$\sigma_{Fe} \sim 20\%$

1.28 ± 0.08

$\sigma_{Ni} \sim 35\%$

(solar units Anders & Grevesse 1989, multi-T *mekal* model)

Distribution of central abundance ratios

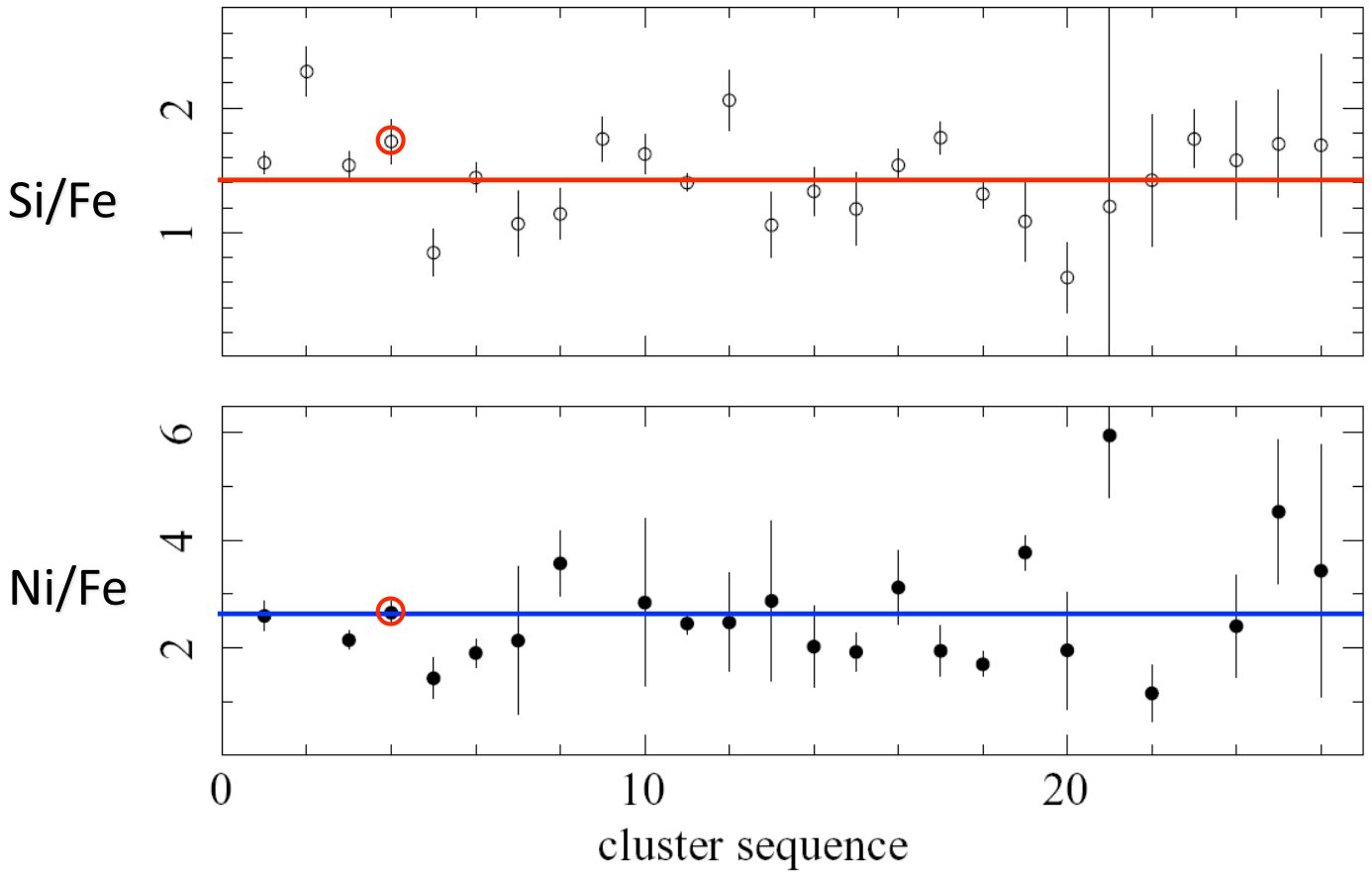

1.47 ± 0.05

$\sigma_{Si/Fe} \sim 20\%$

2.41 ± 0.13

$\sigma_{Ni/Fe} \sim 25\%$

Si/Fe comparison with other samples

Metal	mean	scatter
Si	0.75 ± 0.03	0.22 ± 0.03
Si no Cent.	0.72 ± 0.03	0.17 ± 0.02
Fe	0.51 ± 0.02	0.11 ± 0.01
Fe no Cent.	0.49 ± 0.01	0.07 ± 0.01
Ni	1.28 ± 0.08	0.45 ± 0.06
Ni no Cent.	1.18 ± 0.07	0.34 ± 0.06
Si/Fe	1.47 ± 0.05	0.27 ± 0.05
Si/Fe no Cent.	1.45 ± 0.05	0.30 ± 0.05
Ni/Fe	2.41 ± 0.13	0.60 ± 0.12
Ni/Fe no Cent.	2.40 ± 0.14	0.63 ± 0.13

- Tamura et al. 2004 ✓
  - 15 CC clusters with kT > 3 keV
  - r < 80-100 kpc ~ 0.5 r_{cool}
  - Si/Fe ~ 1.6 ± 0.3
- Rasmussen & Ponmann 2007 ✓
  - Groups of galaxies sample
  - r < 0.08 r_{500} ~ 0.5 r_{cool}
  - Si/Fe = 1.35 $\sigma_{Si/Fe}$ = 32%
- Humphrey & Buote 2006 ✓
  - High L_X Elliptical galaxies sample
  - Si/Fe = 1.50 ± 0.07 $\sigma_{Si/Fe}$ = 16%

Si/Fe comparison with other samples

Metal	mean	scatter
Si	0.75 ± 0.03	0.22 ± 0.03
Si no Cent.	0.72 ± 0.03	0.17 ± 0.02
Fe	0.51 ± 0.02	0.11 ± 0.01
Fe no Cent.	0.49 ± 0.01	0.07 ± 0.01
Ni	1.28 ± 0.08	0.45 ± 0.06
Ni no Cent.	1.18 ± 0.07	0.34 ± 0.06
Si/Fe	1.47 ± 0.05	0.27 ± 0.05
Si/Fe no Cent.	1.45 ± 0.05	0.30 ± 0.05
Ni/Fe	2.41 ± 0.13	0.60 ± 0.12
Ni/Fe no Cent.	2.40 ± 0.14	0.63 ± 0.13

While the moderate spread in the abundance and abundance ratios (Si, Fe, Ni, Si/Fe and Ni/Fe)

➔ suggests similar ICM enrichment processes at work in all clusters cores.

The average Si/Fe ratio nearly constant from the galactic through the group and cluster scales (i.e. small dependence on system mass):

➔ suggests a common enrichment history in all these objects, i.e. a similar mix of SNIa and SNcc.

SNIa vs. SNcc: SN theoretical yields

- O, Ne, Mg from SNcc

- Si, S, Ar, Ca from mix of SNcc-SNIa

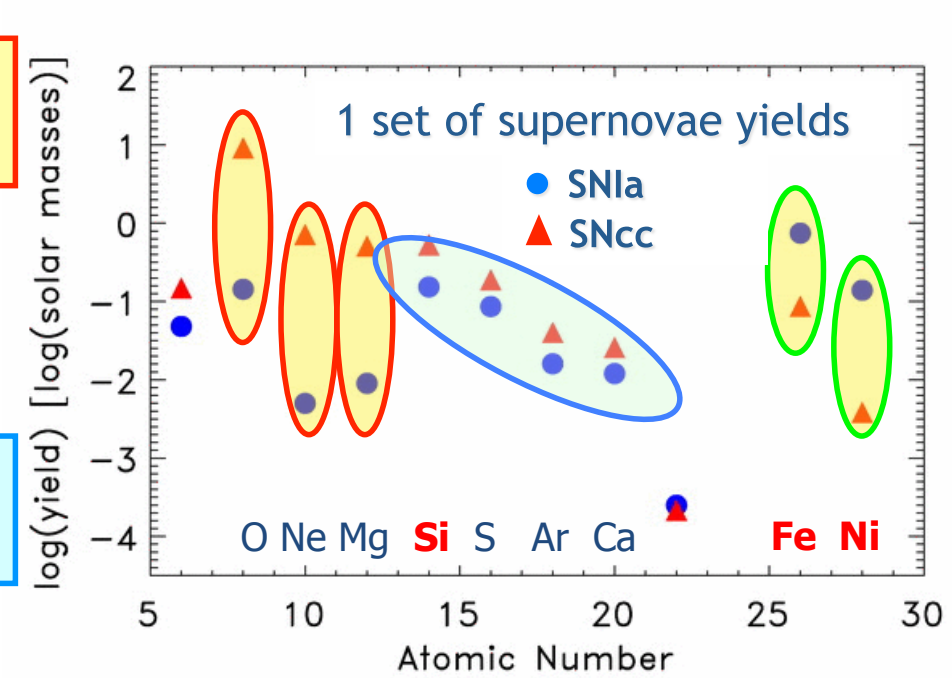

- Fe and Ni mostly from SNIa

Fig from Baumgartner+08

However: in the literature exist a number of works each containing different models (yields). The uncertainties associated to the yields are tens of % (e.g. Gibson et al. 1997), while errors on observed abundance ratios are of ≈ 5%

➔ a robust estimate of SNIa/SNcc should first of all take into account the uncertainties in the yields

SNIa vs. SNcc: the SNIa iron-mass-fraction ξ

- We try to estimate the relative proportion between the two SN types using the observed Si/Fe and Ni/Fe abundance ratios taking into account the uncertainties in the abundance ratios AND in the theoretical yields.

- In general, **the observed X_i/Fe ratio** can be expressed as a linear combination of the theoretical X_i/Fe ratio from SNIa and SNcc:

$$\left(\frac{X_i}{Fe}\right)_{obs} = \xi \cdot \left(\frac{X_i}{Fe}\right)_{SNIa} + (1-\xi) \cdot \left(\frac{X_i}{Fe}\right)_{SNcc}$$

where $\xi = \dfrac{M_{Fe,SNIa}}{M_{Fe,SNIa} + M_{Fe,SNcc}}$ is the **Iron-mass-fraction of SNIa** (that would be needed to enrich the ICM, see Matteucci & Chiappini 05)

We compute ξ by combining a set of 6 SNIa and 7 SNcc yields (SNIa:Iwamoto+99; SNcc:Woosley+95,Chieffi+04,Nomoto+06) **and assuming a 20% errors on the yields**

SNIa vs. SNcc: the SNIa iron-mass-fraction ξ

- The overall permitted range of the SNIa iron-mass-fraction ξ is
  - 0.48 – 0.79 (if 20% unc on yields)
  - 0.55 – 0.73 (if 10% unc on yields)
  - 0.37 - 0.85 (if 30% unc on yields)
  - No substantial differences in the overall range if using *apec* plasma code.

- **From ξ to SNIa number fraction $f = N_{SNIa}/(N_{SNIa}+N_{SNcc})$**
  - Overall permitted range is $f = 0.10 – 0.38$
  - f cannot be reconciled with 0 or 1 (errors of 50% in yields are necessary to have f=0 and errors of 70% to have f=1, which are quite improbable)

➔ **Going beyond the qualitative statement that both SNIa and SNcc contribute to the enrichment of the ICM in the core is quite hard.**

These weak constrains follow from the uncertainties in the yields (almost nothing changed in the yields tables since Gibson+97 contrary to the observed abundance measurements)

SNIa vs. SNcc: Si/Fe radial profiles

➔ variation of Si/Fe with r can be interpreted as evidence for variation of the relative contribution of the two SN types.

Finoguenov et al 2000

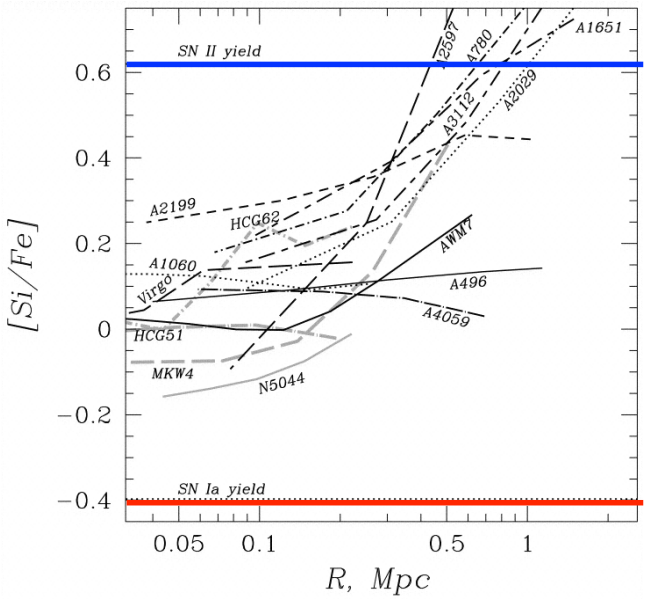

Rasmussen & Ponmann 2007

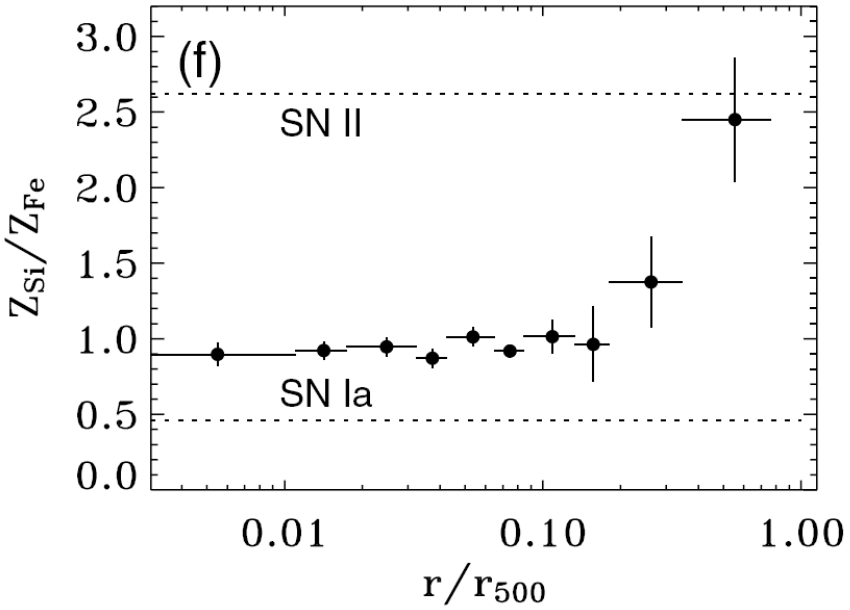

- **Increasing Si/Fe ratio with radius implies a radially increasing predominance of SNcc enrichment in clusters outskirts**

SNIa vs. SNcc: Si/Fe radial profiles

Tamura et al 2004 - XMM

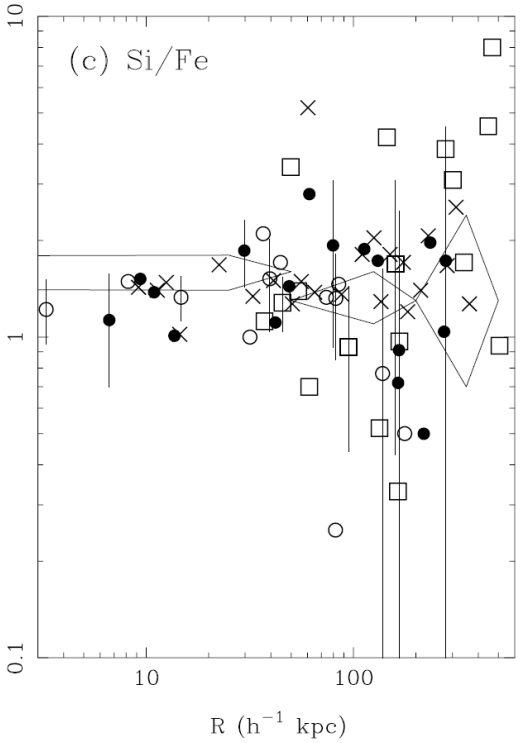

Fabjan et al. 2011

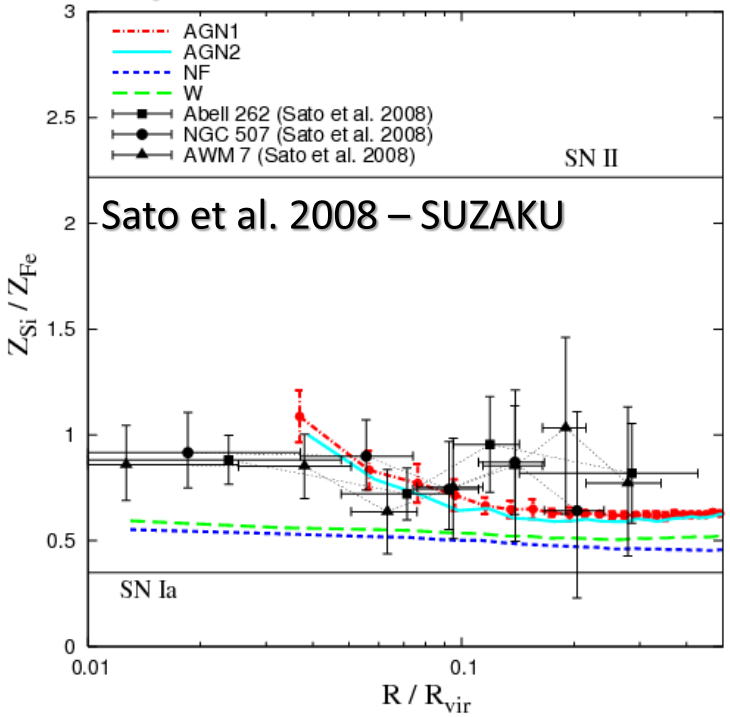

➔ **Constant Si/Fe profiles from XMM and SUZAKU data**: this challenge the "standard picture" where the SNIa from an evolved stellar population are thought to dominate the core enrichment (e.g. McCarty+10, Million+11, Planelles+13).

➔ **The "common" picture where SNIa predominates in cores is outdated.**

Second Part:

The abundance properties of a cool-core cluster @z=1.03

Cluster WARP J1415.1+3612 at z=1.03

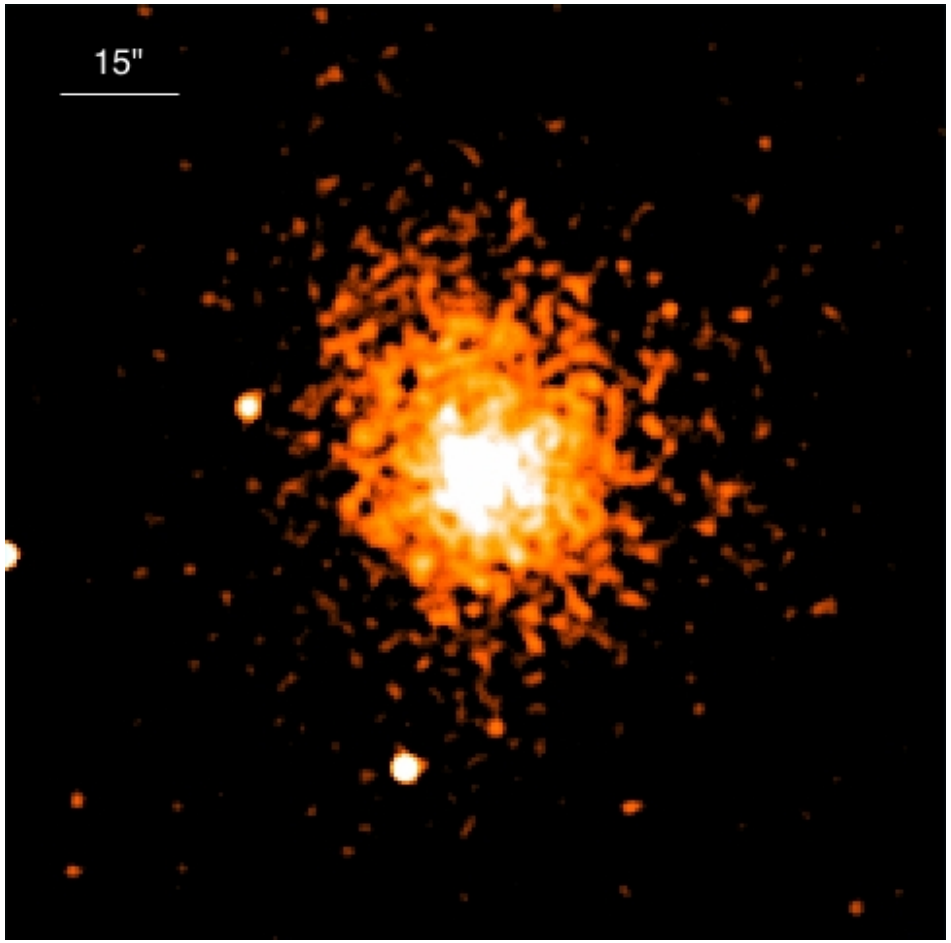

Chandra (ACIS-I and S) observation with total exposure time of 370 ks

Santos, Tozzi, Rosati, Nonino, Giovannini, 2012 A&A 539,105

Cool-Core Clusters in the Local Universe

Perseus cluster Mohr et al. 97

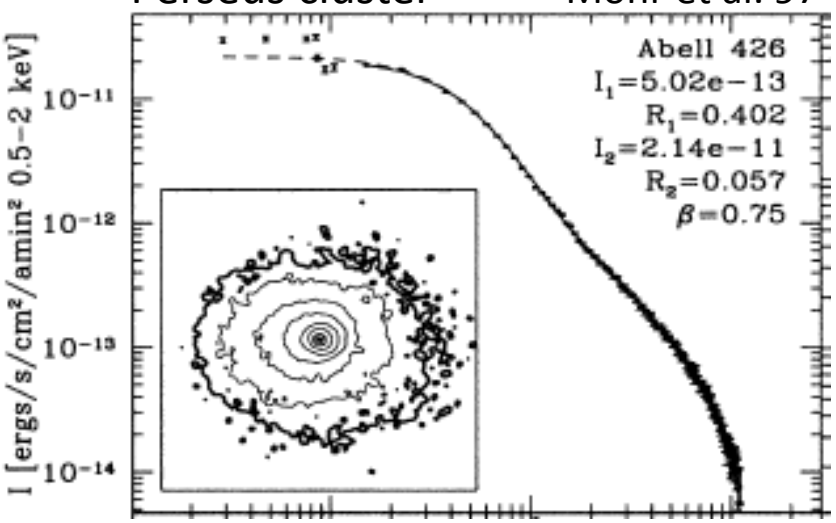

Leccardi & Molendi 08

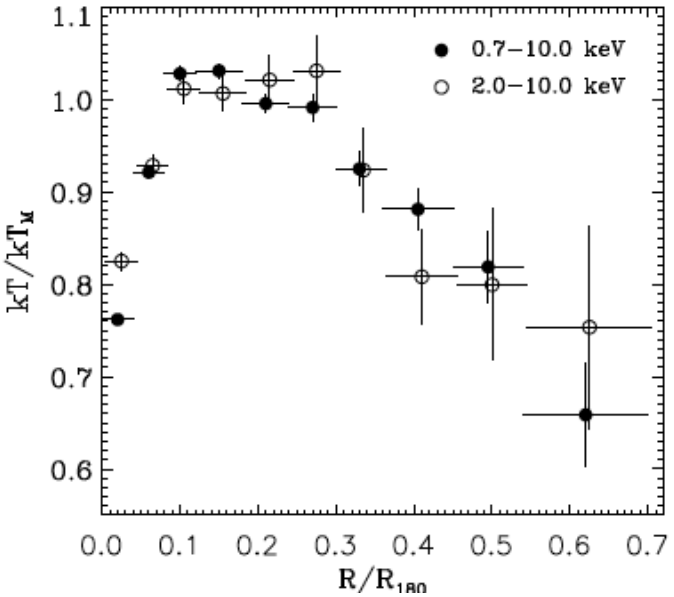

NGC1275

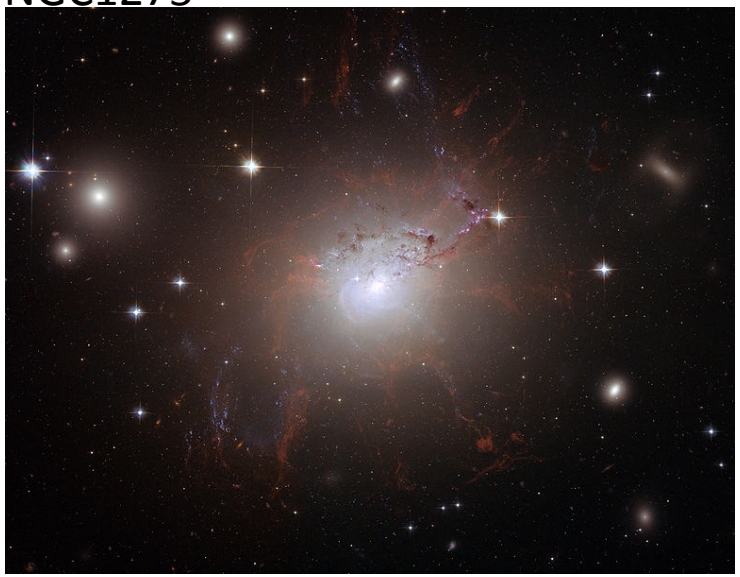

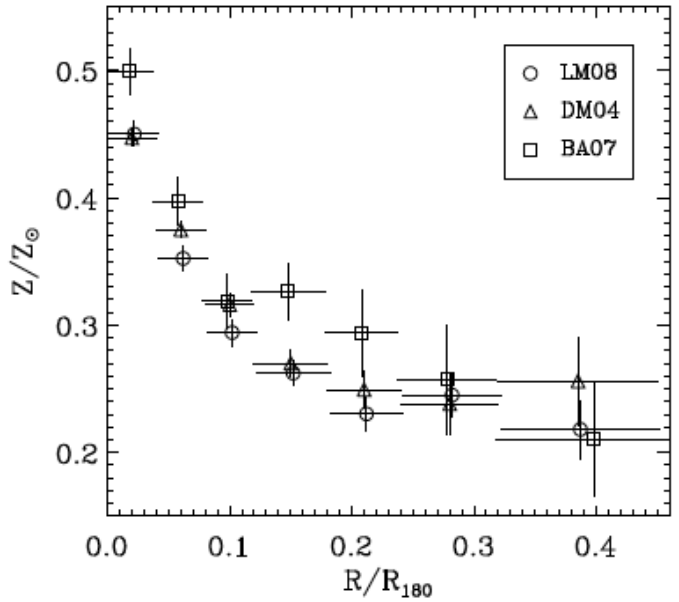

Cluster WARP J1415.1+3612 at z=1

Santos et al. 2012

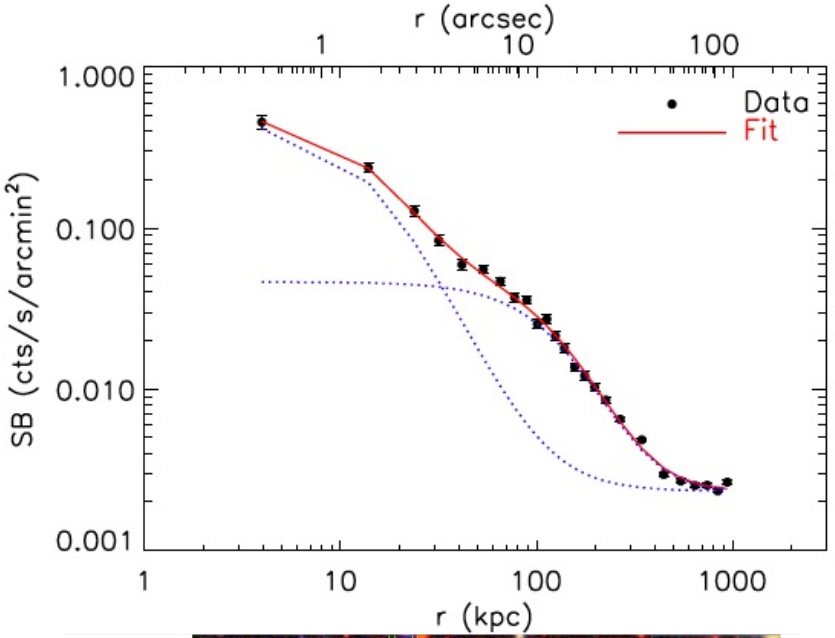

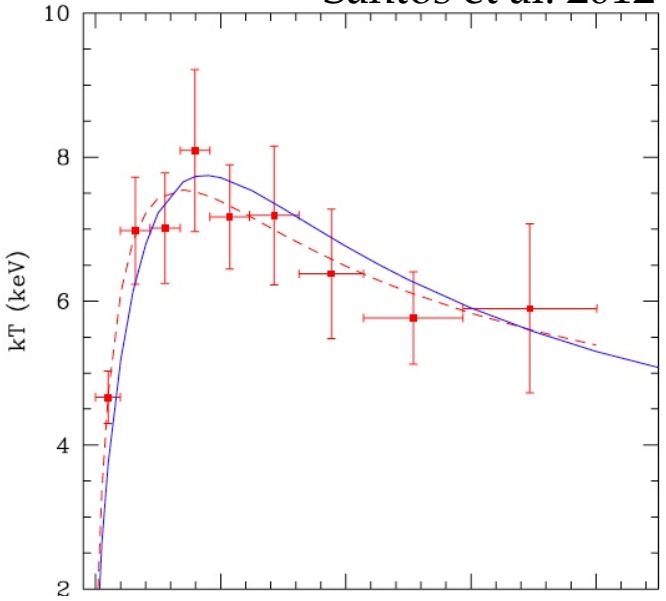

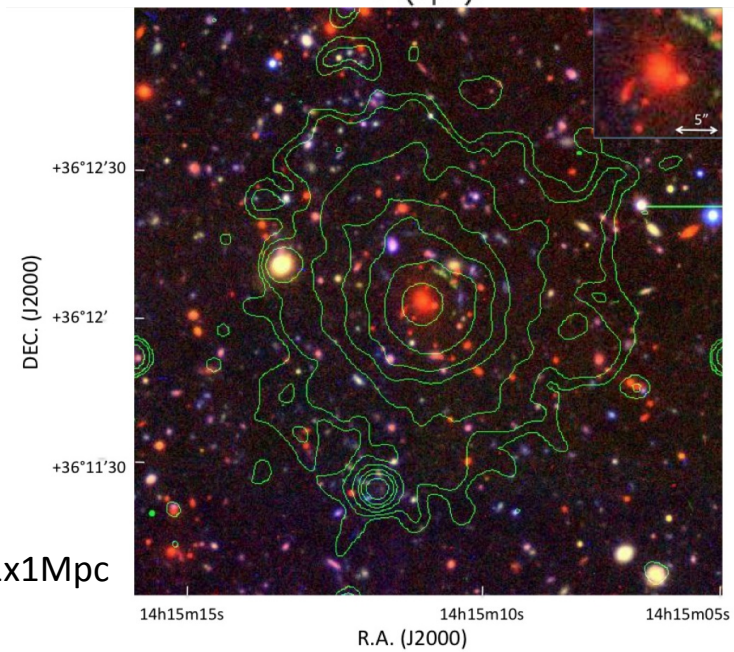

~1x1Mpc

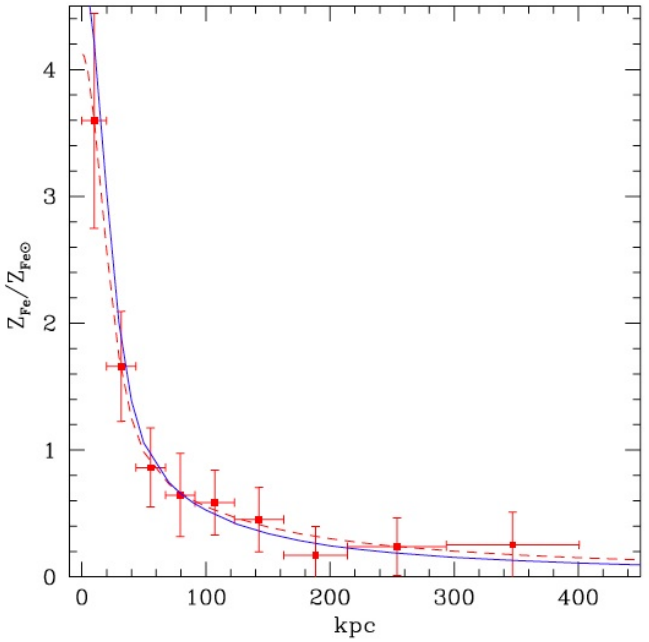

Cluster WARP J1415.1+3612 at z=1

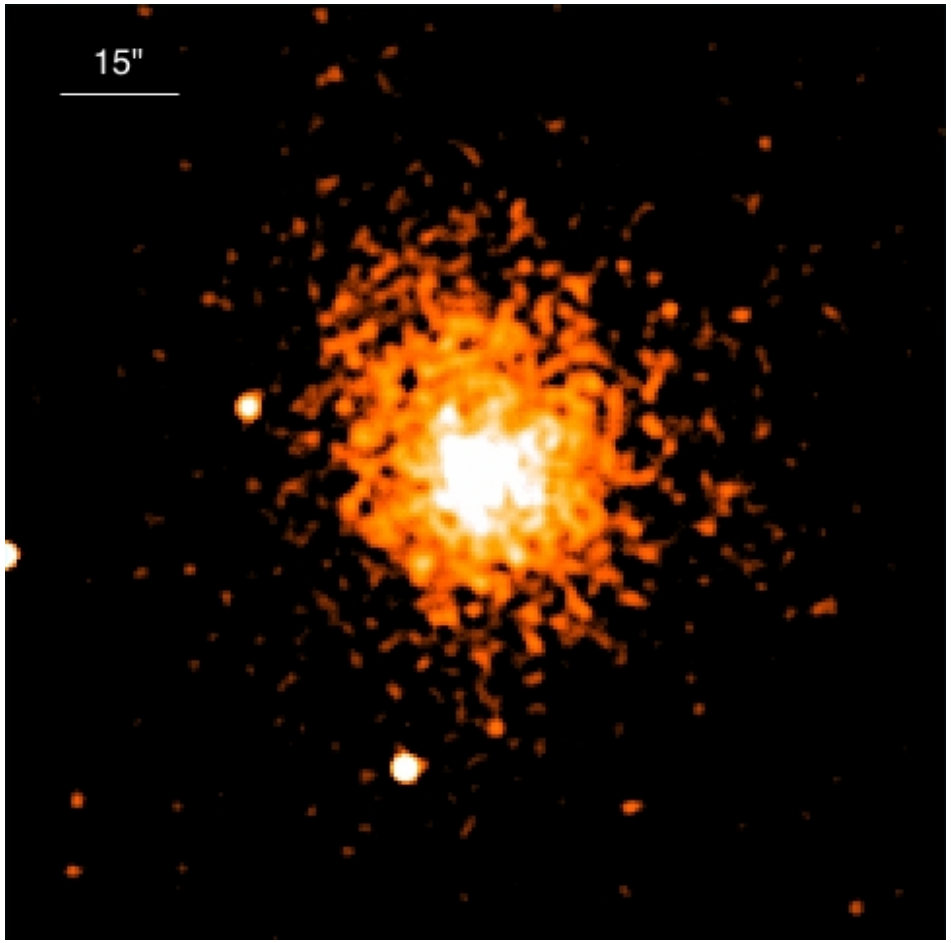

Santos et al. 2012

The analysis of 370 ks Chandra data (ACIS-I and S) shows that WARPJ1415 has all the classical features that characterize nearby cool core clusters.

However:

WARPJ1415 is at z=1.03, i.e. is at the time when the Universe was only 5.8 Gyr old
(~ 42% of the age of the Universe).

Samples and data

WARPJ1415 @z=1.03

- X-ray data: Chandra (Santos et al. 2012)
- Optical data (BCG): high-resolution (0.05”/pix) F775W image provided by the HST-ACS camera and SUBARU data.

Local Cool-Core Clusters @z<0.09:

- First sample:
  - ✧ X-ray data: BeppoSAX: **22 local cluster** (12 CC and 10 NCC) (SD+04).
- Second sample:
  - ✧ X-ray data: XMM archival observations: **Centaurus** (z=0.0114), **A496** (z=0.0329), **A478** (z=0.0881), **A2597** (z=0.0852), **A4059** (z=0.0475), **Hydra-A** (z=0.0539), small sample but representative of the nearby cool-core clusters class.
  - ✧ Optical data (BCGs): NIR K-band imaging (SOFI at 2.2m telescope at La Silla)

Iron Mass and Iron Mass excess

The Fe Mass enclosed within a certain radius r′ is:

$$M_{Fe}(<r') \equiv \int_0^{r'} \rho_{Fe}(r)\,dV(r)$$

We compute the Fe mass within Δ2500 (317^{+22}_{-18} kpc for WARPJ1415)

We define the Fe abundance "excess": $Z^{exc}_{Fe}(r) = Z_{Fe}(r) - Z_{Fe}(r/r_{200} > 0.2)$

The Fe Mass "excess":

$$M^{exc}_{Fe}(<r') \propto 4\pi \int_0^{r'} Z^{exc}_{Fe}(r) n_{gas}(r)\, r^2 dr$$

Abundance profiles

- LEC Low Entropy Core (CC)
- MEC Medium Entropy Core
- HEC High Entropy Core (NCC)

Cool Core region
$R < 0.1R_{180}$

Intermediate region
$0.1R_{180} < R < 0.2R_{180}$

Outer region
$R > 0.2R_{180}$ $Z \sim 0.24$

Leccardi et al. 2010

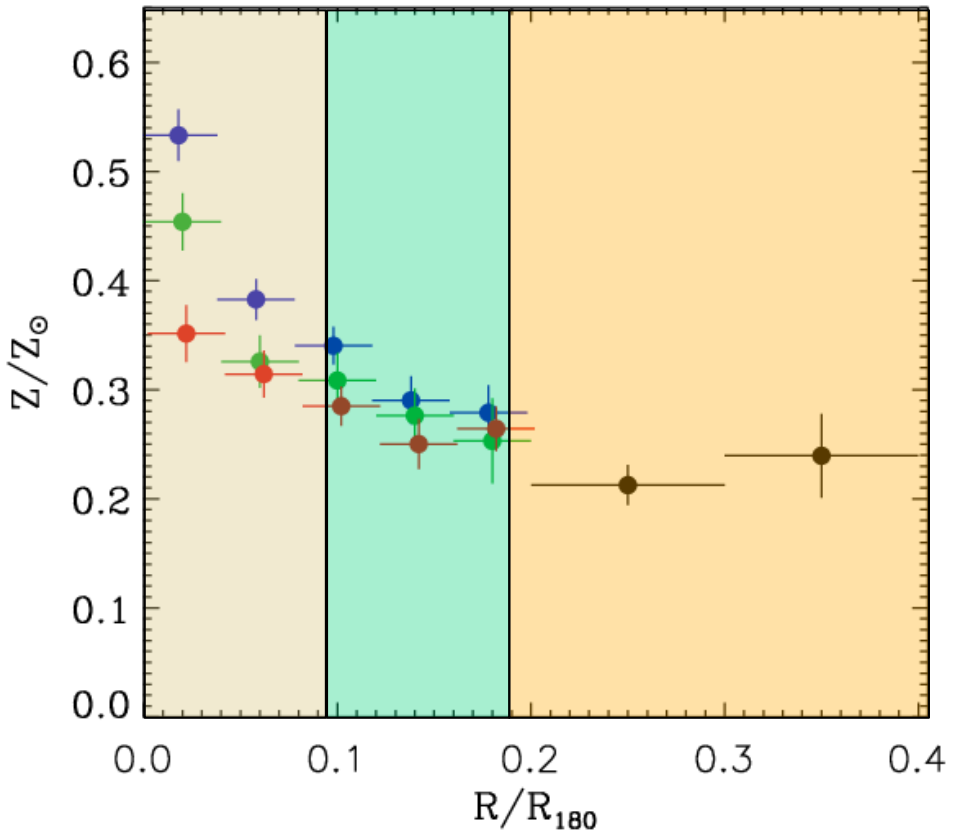

A NOTE OF CAUTION: the Fe abundance excess extends out to ~0.2 r/r_{180}
taking smaller radii will lead to an underestimates of the iron mass in the excess
and to incorrect estimate of its properties
(see e.g. Boehringer+04, David & Nulsen 08, that used fixed aperture of 50 kpc to estimate Fe excess)

Comparison with Local Clusters

SAX (black) + XMM (blue)

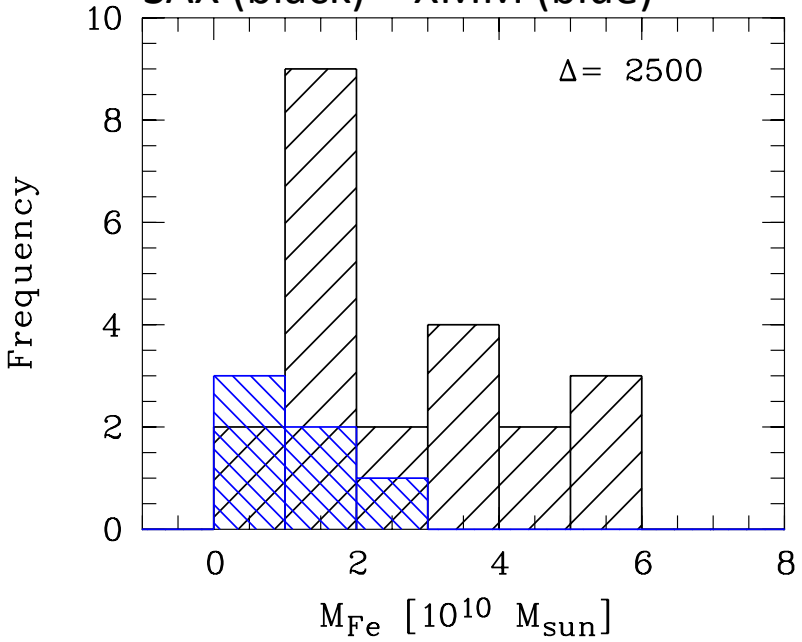

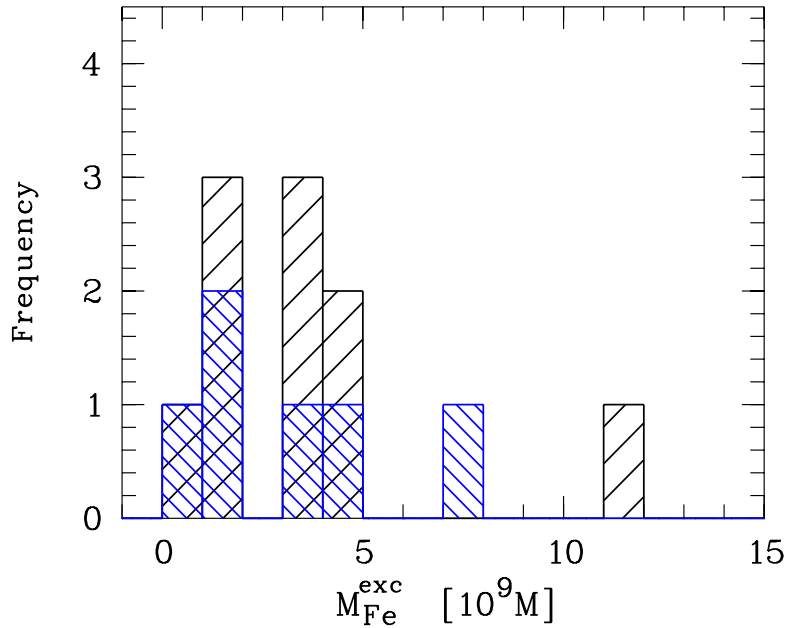

Fe Mass in the ICM of Local Clusters (@Δ=2500): $M_{Fe} \approx 0.5 \div 6 \times 10^{10} M_{\odot}$

Fe Mass Excess in CC Local Clusters: $M_{Fe}^{exc} \approx 1 \div 10 \times 10^{9} M_{\odot}$

In local CC the Fe mass excess in CC is $\sim 20\%$ of the total ICM Fe mass within r_{2500}

Comparison with Local Clusters

SAX (black) + XMM (blue)

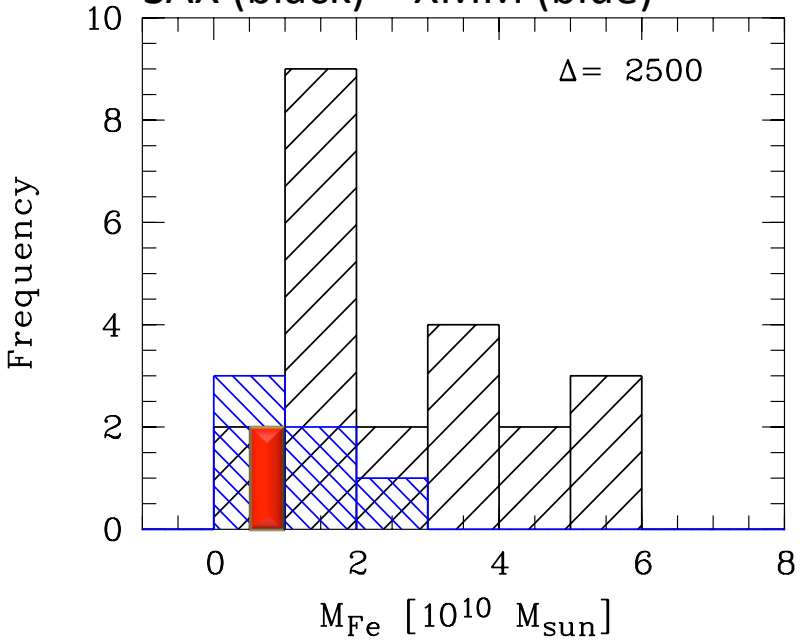

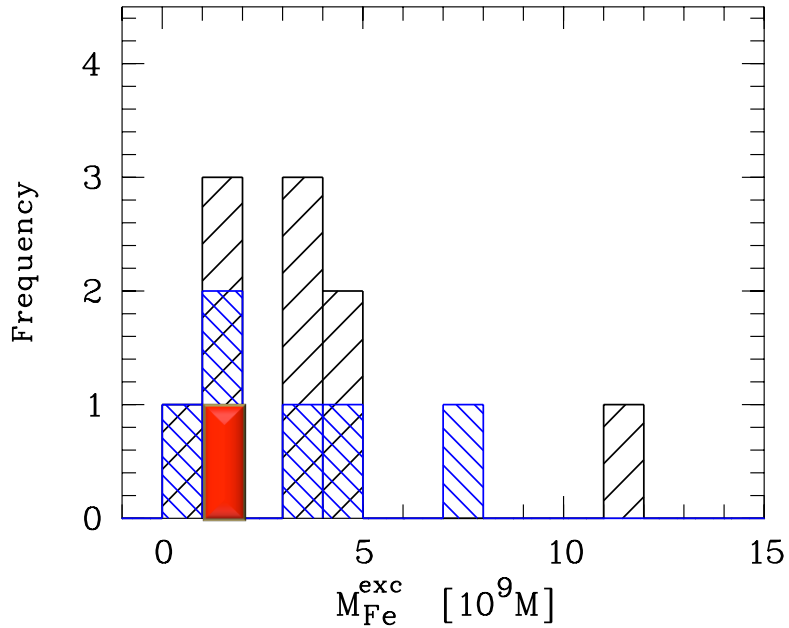

Fe Mass in the ICM of Local Clusters (@Δ=2500): $M_{Fe} \approx 0.5 \div 6 \times 10^{10} M_{\odot}$

WARPJ1415 (@Δ=2500) : $M_{Fe} \approx (0.76 \pm 0.13) \times 10^{10} M_{\odot}$

Fe Mass Excess in CC Local Clusters: $M_{Fe}^{exc} \approx 1 \div 10 \times 10^{9} M_{\odot}$

WARPJ1415: $M_{Fe}^{exc} \approx (1.7 \pm 0.4) \times 10^{9} M_{\odot}$

In local CC the Fe mass excess in CC is $\sim 20\%$ of the total ICM Fe mass within r_{2500}

WARPJ1415: $\approx 0.22 \pm 0.06$

Comparison with Local Clusters

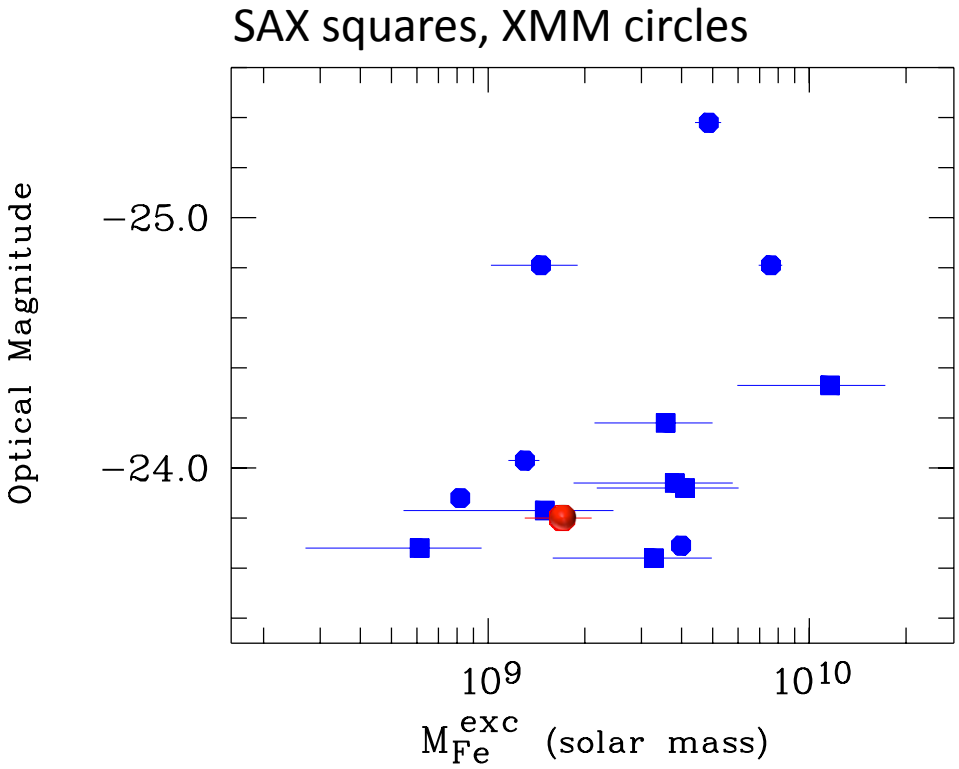

BCG in WARPJ1415:

very large, luminous, massive galaxy spatially coincident with the peak of the X-ray emission

$L_B = 3 \times 10^{11} L_{B\odot}$

$M_\star = 2 \times 10^{12} M_\odot$ (Fritz et al. 2009)

$M_{Rc} = -23.8$ mag (Santos et al. 2012)

We assume that the Fe in the excess was originated by the stars that are currently forming the BCG. Indeed in cool core clusters:

- a BCG is omnipresent and coincident with the peak of the Fe abundance
- in SD+04 we found the consistency of the Fe Mass excess with being produced by stars associated with the BCG (we used Bruzual & Charlot 03, Pipino+02)

Z_{Fe} peak formation time scale

- The Fe mass excess in WARPJ1415, similar to those of Local CC clusters, suggests that the enrichment process that produced the Fe excess occurred in an early phase, i.e. at z > 1.

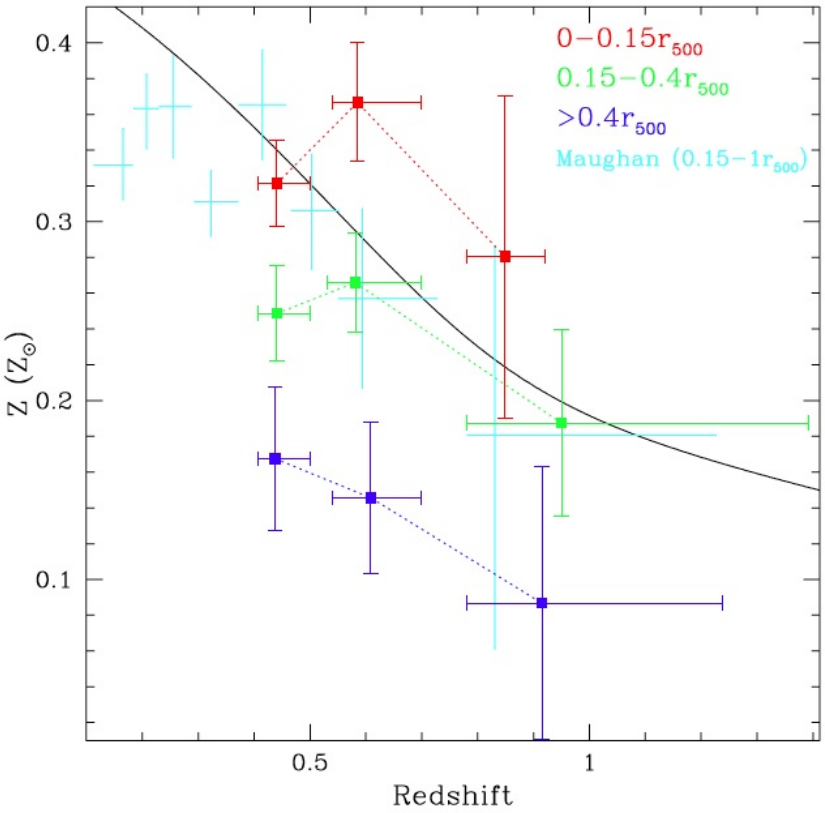

Baldi+12 (39 gcl): mean weighted Fe abundance as a function of z in different spatial bins:

The mean Z_{Fe} within 0.15 r_{500} for clusters within **0.4 < z < 1.** is consistent with being constant (Z_{Fe}~ 0.3 $Z_{\odot}$)

Santos+08,10:

The SB concentration parameter c_{SB}: SB(r<40 kpc) / SB(r<400 kpc) up to z~1.4 shows only moderate evolution

Z_{Fe} peak formation time scale

- The Fe mass excess in WARPJ1415, similar to those of Local CC clusters, suggests that the enrichment process that produced the Fe excess occurred in an early phase, i.e. at z > 1.

- We compute the Iron peak formation time scale from eq. (see Boehringer et al. 04):

$$t_{enrich} = M_{Fe}^{exc}\left[L_B^{BCG}(SNR \times 10^{-12} L_{B_\odot}^{-1})\eta_{Fe}\right]^{-1}$$

with

M_{Fe}^{exc}	$= 1.7 \times 10^9 M_\odot$	from WARPJ1415 at z=1.
L_B^{BCG}	$= 3 \times 10^{11} L_{B,\odot}$	(Fritz et al. 09)
SNR	$= 0.50 \pm 0.23$ SNu	(Barbary et al. 12 for SNIa in gcl at 0.9 < z < 1.46)
η_{Fe}	$=$ Fe yield per SNIa $= 0.7 M_\odot$	(Iwamoto et al. 1999)

Z_{Fe} peak formation time scale

- The Fe mass excess in WARPJ1415, similar to those of Local CC clusters, suggests that the enrichment process that produced the Fe excess occurred in an early phase, i.e. at z > 1 (see also Baldi et al. 2012).

- We compute the Iron peak formation time scale from eq. (see Boehringer et al. 04):

$$t_{enrich} = M_{Fe}^{exc}\left[L_B^{BCG}(SNR \times 10^{-12} L_{B_\odot}^{-1})\eta_{Fe}\right]^{-1}$$

with M_{Fe}^{exc}	$= 1.7 \times 10^9 M_\odot$	from WARPJ1415 at z=1.
L_B^{BCG}	$= 3 \times 10^{11} L_{B,\odot}$	(Fritz et al. 09)
SNR	$= 0.50 \pm 0.23$ SNu	(Barbary et al. 12 for SNIa in gcl at 0.9 < z < 1.46)
η_{Fe}	$=$ Fe yield per SNIa $= 0.7 M_\odot$	(Iwamoto et al. 1999)

$$t_{enrich} \approx 16.2\ Gyr\ >>\ t_{H(z=1)} = 5.9\ Gyr$$

➡ The observed SNR for galaxy clusters up to z~1.5 fails to reproduce the Z_{Fe} peak

SN Rate from the Z_{Fe} peak

- We can constrain the SN Rate required to reproduce the Fe abundance peak

$$SNR_{SNIa} = \frac{M_{Fe}^{exc} \times 10^{12} L_{B\odot}}{L_B^{BCG} \Delta t_{enrich} \eta_{Fe}}$$

SN Rate from the Z_{Fe} peak

- We can constrain the SN Rate required to reproduce the Fe abundance peak

$$SNR_{SNIa} = \frac{M_{Fe}^{exc} \times 10^{12} L_{B\odot}}{L_B^{BCG} \Delta t_{enrich} \eta_{Fe}}$$

- Assuming that most of SF in WARPJ1415's BCG occurred starting from

$$2 \leq z < 3$$ (e.g. Renzini 06, Daddi+04, Rosati+09)

the time scale to build up the Fe abundance peak in WARPJ1415 at z=1. is:

$$2.4\ Gyr \leq \Delta t_{enrich} < 3.6\ Gyr$$

SN Rate from the Z_{Fe} peak

- We can constrain the SN Rate required to reproduce the Fe abundance peak

$$SNR_{SNIa} = \frac{M_{Fe}^{exc} \times 10^{12} L_{B\odot}}{L_B^{BCG} \Delta t_{enrich} \eta_{Fe}}$$

- Assuming that most of SF in WARPJ1415's BCG occurred starting from

$$2 \leq z < 3$$ (e.g. Renzini 06, Daddi+04, Rosati+09)

the time scale to build up the Fe abundance peak in WARPSj1415 at z=1. is:

$$2.4\ Gyr \leq \Delta t_{enrich} < 3.6\ Gyr$$

We obtain:

$$\boxed{SNR_{SNIa} \approx 2.2 - 3.4\ SNu}$$

➡ The required SNR are >> than the observed ones (eg 0.5±0.2 SNu Barbary+12)

Z_{Fe} peak build up

- How can we get such a high SN Rate ?

  - ✧ We have observational evidences that the Star Formation Rate (SFR) during the period of the assembly of the BCG can be extremely high (e.g. Spiderweb galaxy at z=2 with SFR=1390 ± 150 $M_{\odot}$ yr^{-1}, Seymour+12)

Z_{Fe} peak build up

- How can we get such a high SN Rate ?

  - ✧ We have observational evidences that the Star Formation Rate (SFR) during the period of the assembly of the BCG can be extremely high (e.g. Spiderweb galaxy at z=2 with SFR=1390 ± 150 $M_\odot$ yr^{-1}, Seymour+12)

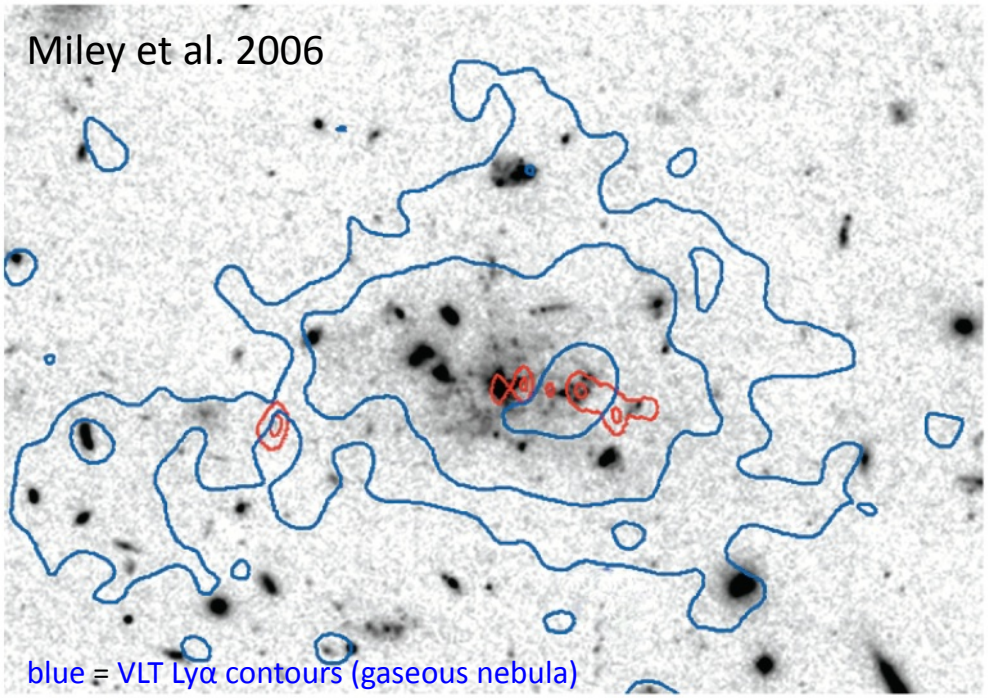

blue = VLT Lyα contours (gaseous nebula)
red = VLA 8GHz contours (non-thermal emission)
grey = HST ACS image

This massive system is in a special phase of rapid central BH and host galaxy growth, likely caused by a gas-rich merger in a dense environment.

The gaseous nebula extends for > 200 kpc
≈ size of envelopes of local cD galaxies

➔Expected SNR much higher that the SNR observed up to z=1.5

Z_{Fe} peak build up

- How can we get such a high SN Rate ?

  - ✧ We have observational evidences that the Star Formation Rate (SFR) during the period of the assembly of the BCG can be extremely high (e.g. Spiderweb galaxy at z=2 with SFR=1390 ± 150 $M_{\odot}$ yr^{-1}, Seymour+12)

  - ✧ We also know that the ~50-60% of the Iron released by SNIa explosions occurs within ~ 1 Gyr (e.g. Maoz et al. 10/12 and ref. therein)

Z_{Fe} peak build up

- How can we get such a high SN Rate ?

  - ✧ We have observational evidences that the Star Formation Rate (SFR) during the period of the assembly of the BCG can be extremely high (e.g. Spiderweb galaxy at z=2 with SFR=1390 ± 150 $M_\odot$ yr^{-1}, Seymour+12)

  - ✧ We also know that the ~50-60% of the Iron released by SNIa explosions occurs within ~ 1 Gyr (e.g. Maoz et al. 10/12 and ref. therein)

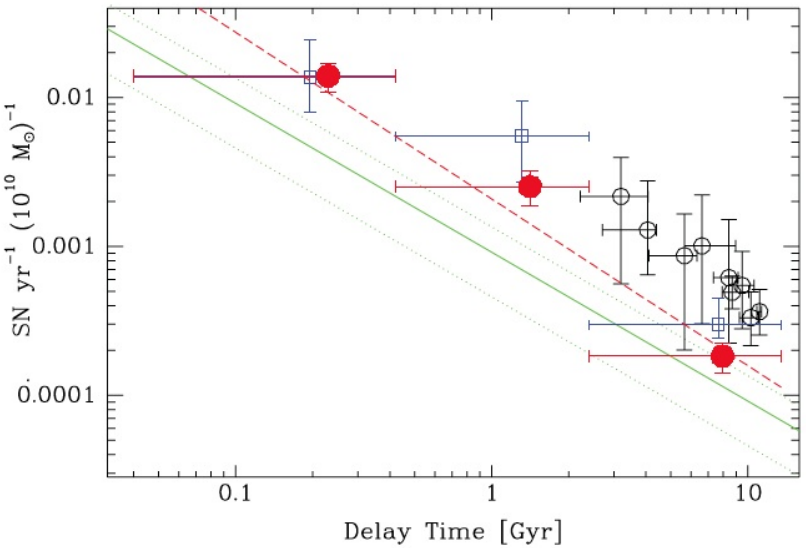

Delay Times Distribution from SDSSII (Maoz, Mannucci & Brandt 2012)

Z_{Fe} peak build up

- How can we get such a high SN Rate ?

  - ✧ We have observational evidences that the Star Formation Rate (SFR) during the period of the assembly of the BCG can be extremely high (e.g. Spiderweb galaxy at z=2 with SFR=1390 ± 150 $M_{\odot}$ yr^{-1}, Seymour+12)

  - ✧ We also know that the ~50-60% of the Iron released by SNIa explosions occurs within ~ 1 Gyr (e.g. Maoz et al. 10/12 and ref. therein)

➡ We propose that the bulk of the Iron Excess in WARPJ1415 was likely produced by the prompt release of the SNIa just after the BCG assembly.

This is contrary to the "common" picture where the Z_{Fe} peak form slowly after the BCG formation.

How Do The Iron And The BCG Stellar Light Radial Distributions Compare?

We compute the metal abundance excess profile "expected" when the metal excess distribution traces the light distribution of BCG.

Hypothesis: We assume that the Iron density excess distribution, $n_{Fe}(r)$, follows the star light distribution of the BCG, $l(r)$, i.e.: $n_{Fe}(r) \propto l(r)$

Therefore:

$$Z_{Fe}(r) = n_{Fe}(r)/n_H(r) \propto l(r)/n_H(r)$$

and compute the Fe abundance excess profile expected under this hypothesis .

The projected abundance excess Z_{proj} measured within a bin with bounding radii b_{min} and b_{max} is related to the de-projected metal abundance-excess distribution $Z(r)$ by the following equation (see SD & Molendi 01):

$$Z_{\rm proj}(b_{\rm min}, b_{\rm max}) = \frac{\int_{b_{\rm min}}^{b_{\rm max}} b\,db \int_{b^2}^{\infty} \{[n^2(r)Z(r)]/\sqrt{r^2 - b^2}\} dr^2}{\int_{b_{\rm min}}^{b_{\rm max}} b\,db \int_{b^2}^{\infty} \{[n^2(r)]/\sqrt{r^2 - b^2}\} dr^2}$$

Predicted vs. observed Fe excess profiles

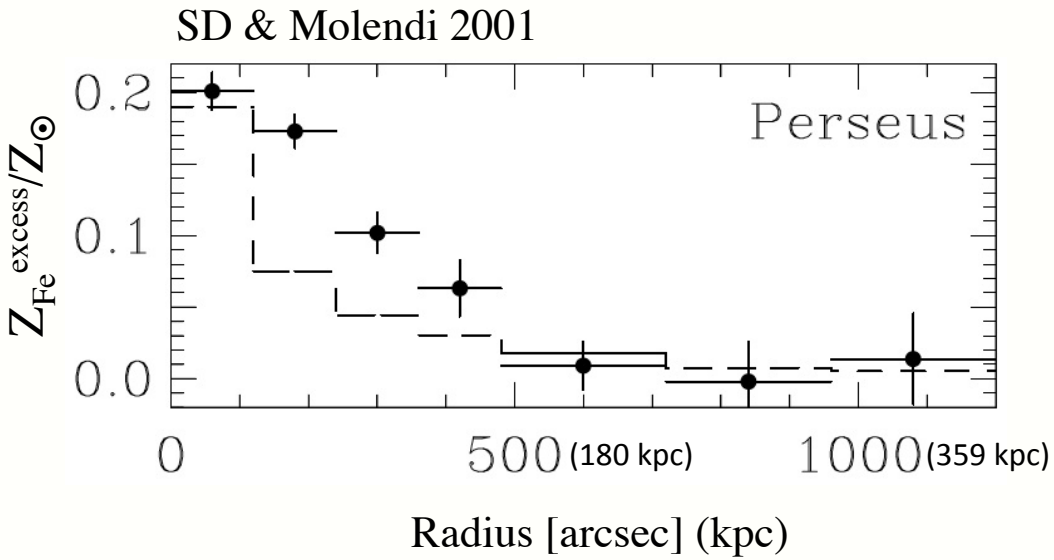

We found that the real Fe excess distribution was broader than the expected one.

(see similar results in e.g., Matsushita et al. 03/04, Churazov et al. 03, Rebusco et al. 05, David & Nulsen 08)

This is an indication that the Iron produced by the BCG moved away from the place of origin

We repeated this exercise with new X-ray and optical data for WARPJ1415 at z=1 and a small sample of local cool-core clusters.

Predicted vs. observed Z_{Fe} excess profiles

XMM Local Cluster Sample : z<0.09

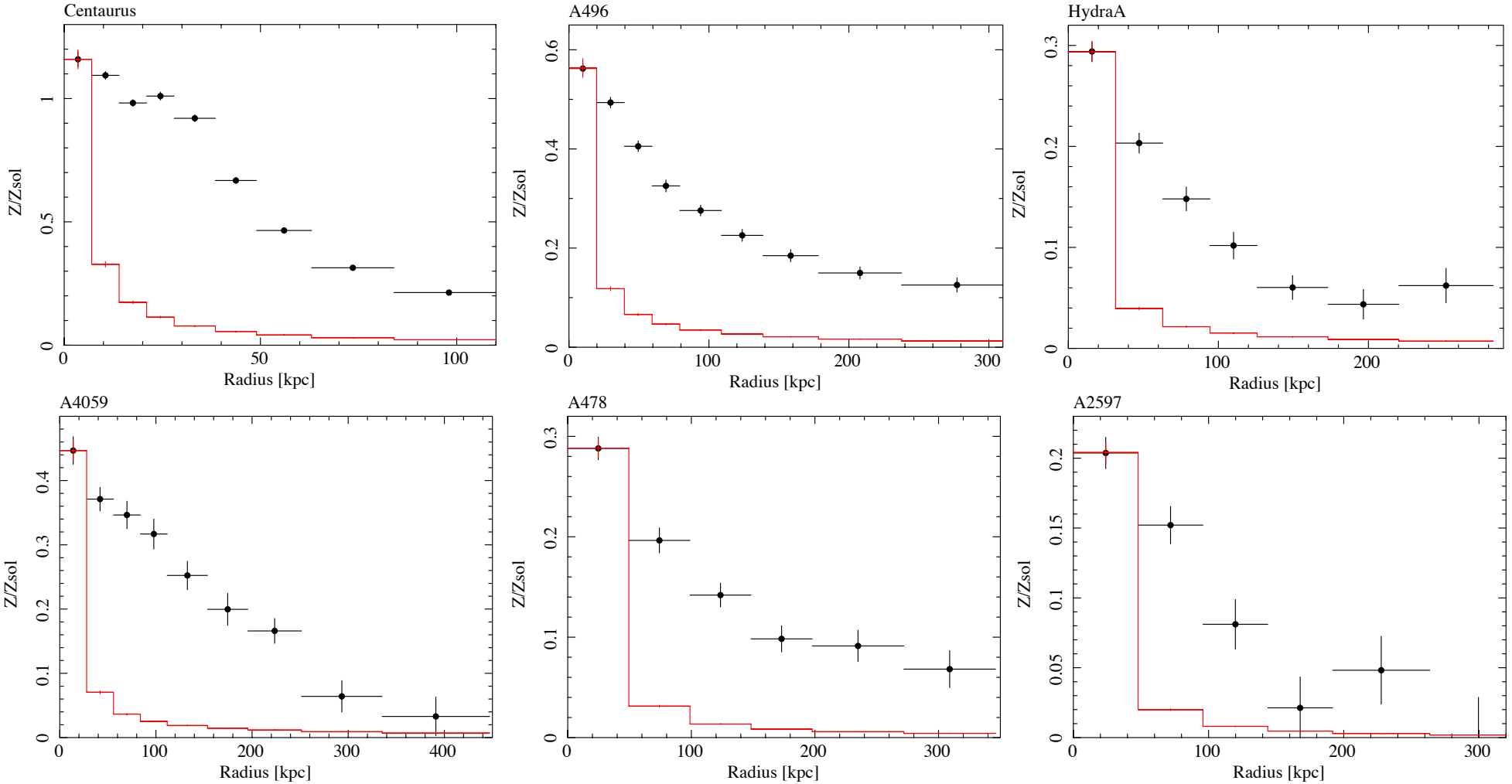

Predicted vs. observed Z_{Fe} excess profiles

WARPJ1415:

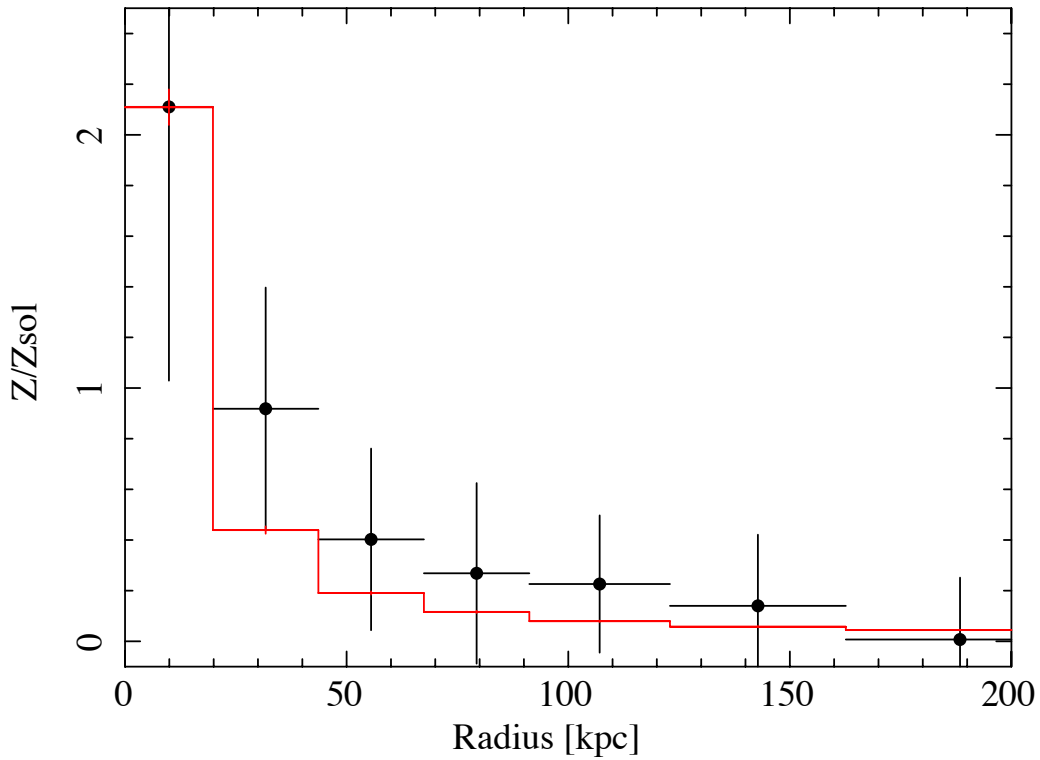

The Fe abundance excess profile of WARPJ1415 is more similar to the BCG optical light profile than in local cool-core clusters.

Relative Differences btw. observed and predicted Z_{Fe} excess profiles

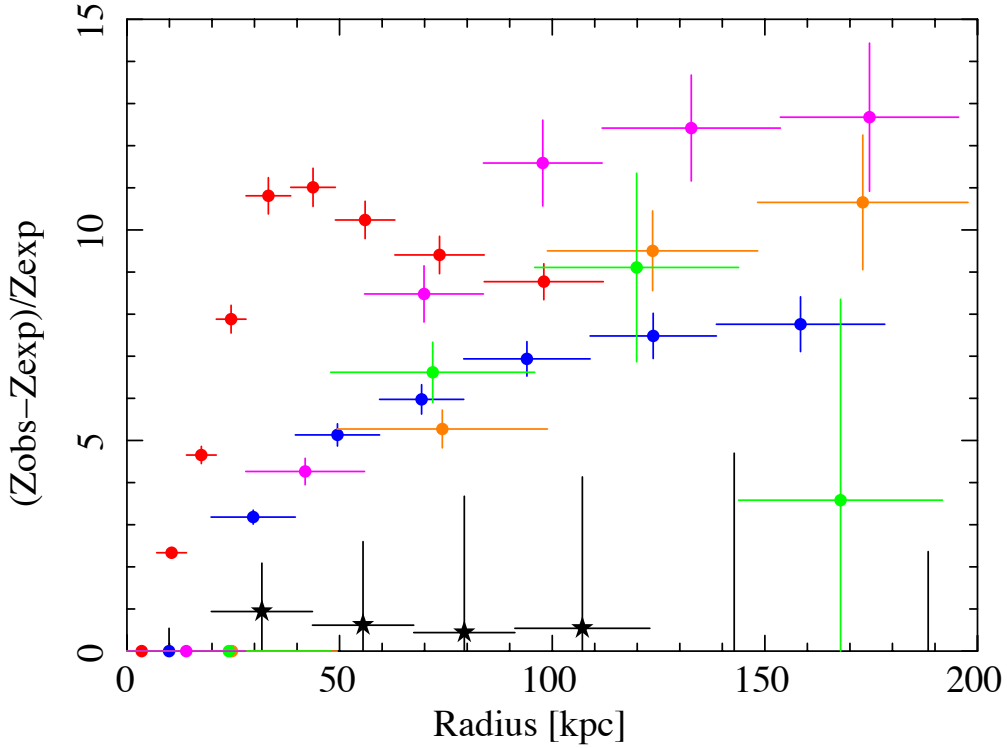

- The observed Z_{Fe} excess profile in WARPJ1415 is close to the predicted
- This differs significantly from what it is observed in local CC clusters, where the Z_{Fe} excess profiles are broader than the expected ones.

Relative Differences btw. observed and predicted Z_{Fe} excess profiles

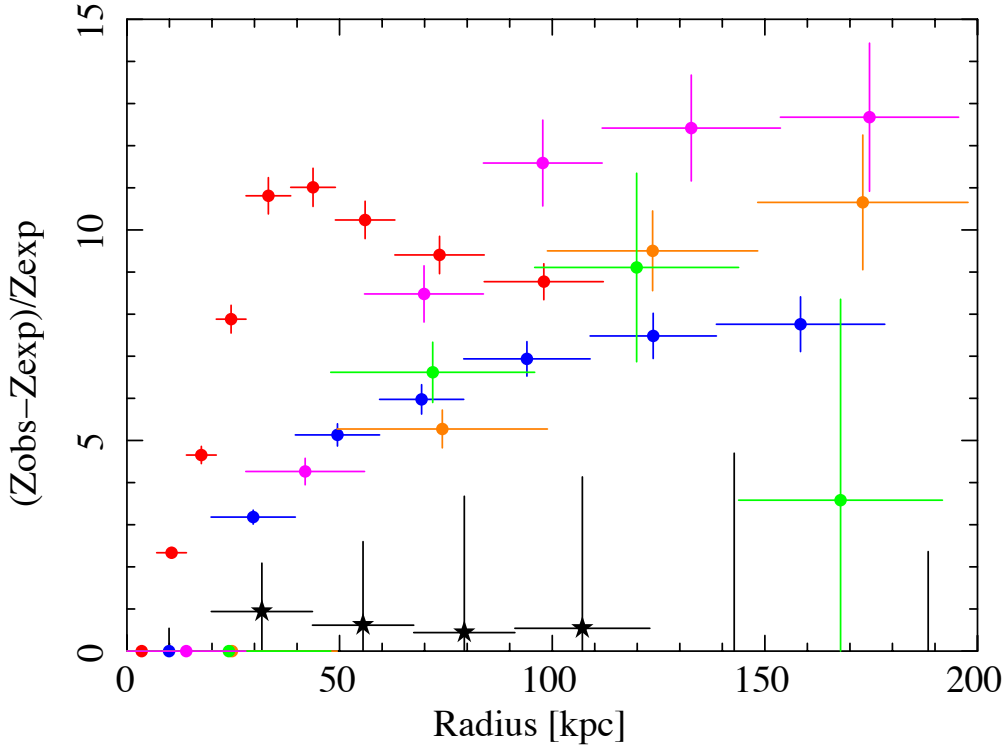

- If WARPJ1415 can be considered a representative massive CC cluster at z=1, then this difference can be explained by assuming that mixing mechanisms (e.g. AGN driven turbulence, mergers, etc.) have broadened the Fe abundance profile from z~1.
- The Iron peak broadening time scale is ≥ 7.9 Gyr (i.e. the look back time at z=1.03).

Metal-enriched Outflows Driven By AGN

Kirkpatrick et al. 2011: 10 clusters observed with *Chandra.*

The BCGs have experienced recent AGN activity in the forms of bright radio emission, cavities, and shock fronts embedded in the ICM.

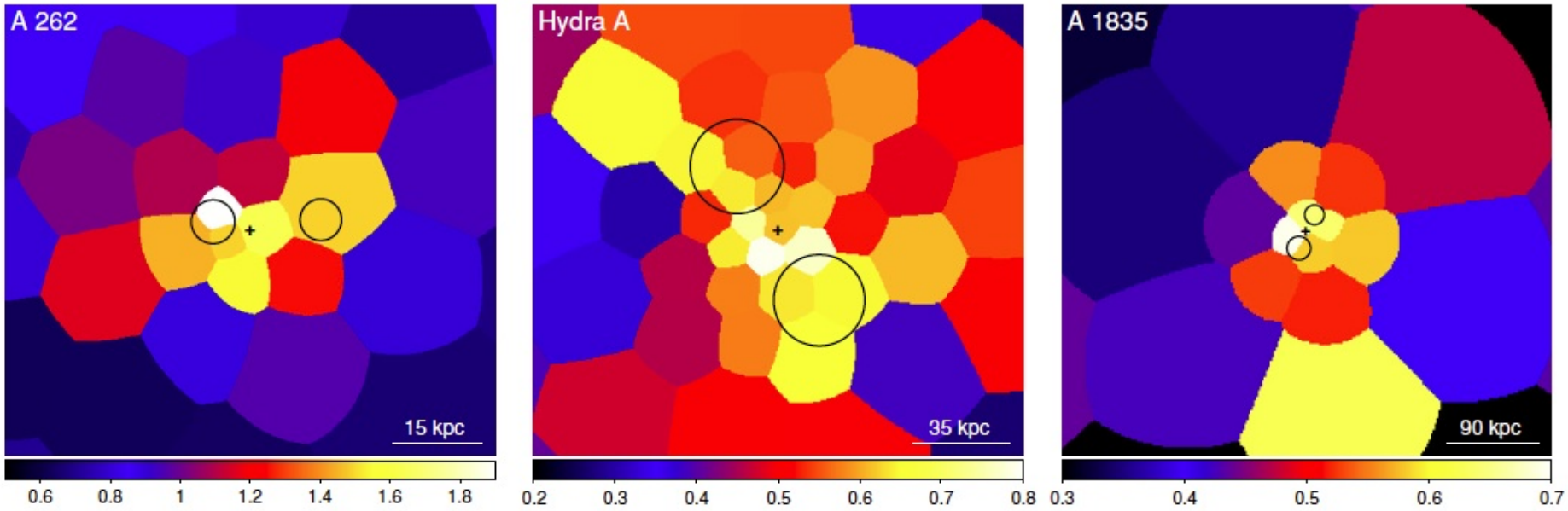

- The heavy elements are distributed anisotropically and are aligned with the large-scale radio and cavity axes.
- They are apparently being transported from the halo of the BCG into the ICM along large-scale outflows driven by the radio jets.
- see also Simionescu+08,09; Gitti +11; Kirkpatrick+09; O'Sullivan+11

Metal-enriched Outflows Driven By AGN

Kirkpatrick et al. 2011: 10 clusters observed with *Chandra.*

The BCGs have experienced recent AGN activity in the forms of bright radio emission, cavities, and shock fronts embedded in the ICM.

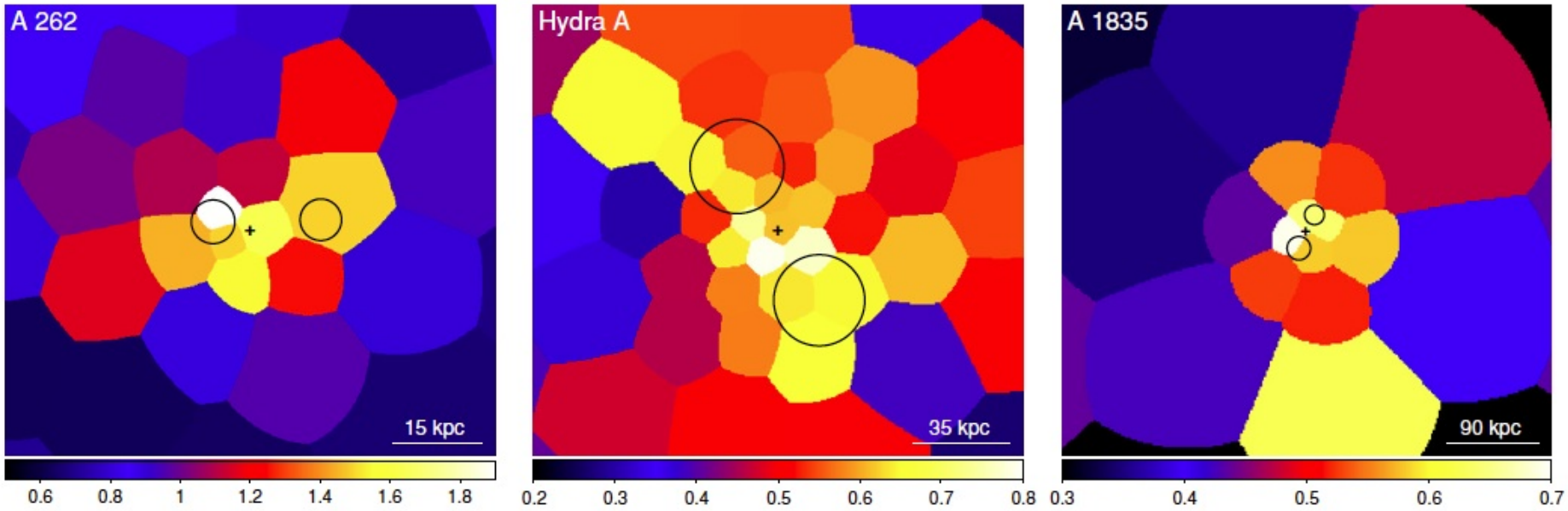

- McNamara+13: a 5x10^10 solar mass outflow of molecular gas launched by radio bubbles in the A1835 BCG ➔ radio-mechanical feedback not only heats ICM surrounding the BCG but it's able to sweep higher density molecular gas away from cluster centers.

Metals in a sloshing scenario

- Minor mergers can develope Cold Fronts in Cool Core clusters due to gas sloshing.
- In this case the temperature map in the core shows a typical spiral-like pattern.
- The T and Z_{Fe} sharply drop across the cold fronts and Z_{Fe} is high in the spiral

Temperature

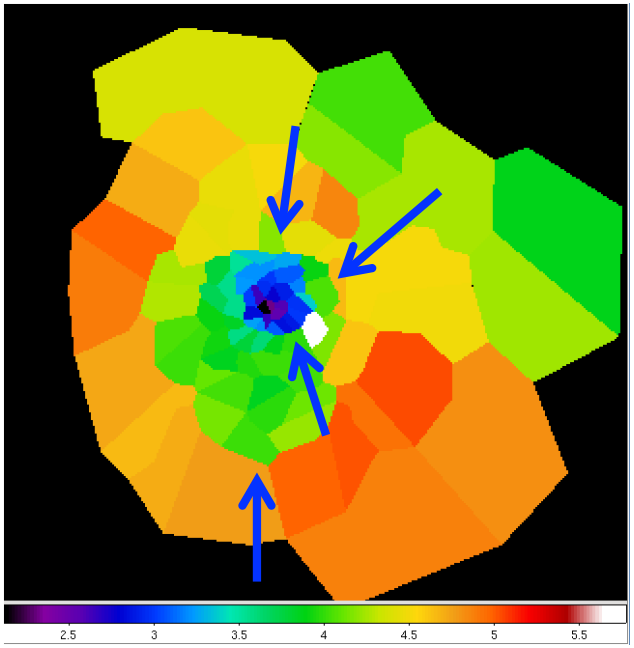

Iron Abundance

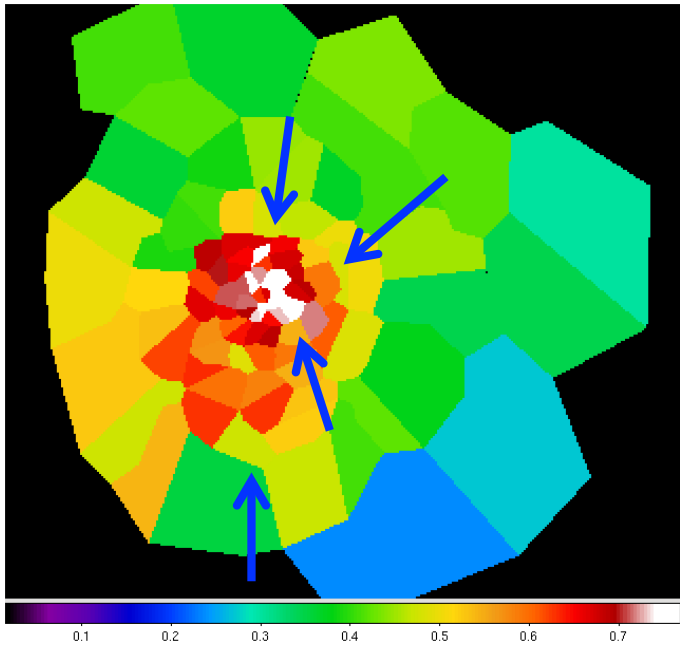

Ghizzardi, SD et al. 2013: Abell 496 XMM data

(see also e.g., Roediger+11, Simionescu+10)

Metals in a sloshing scenario

- Minor mergers can develope Cold Fronts in Cool Core clusters due to gas sloshing.
- In this case the temperature map in the core shows a typical spiral-like pattern.
- The T and Z_{Fe} sharply drop across the cold fronts and Z_{Fe} is high in the spiral

Temperature

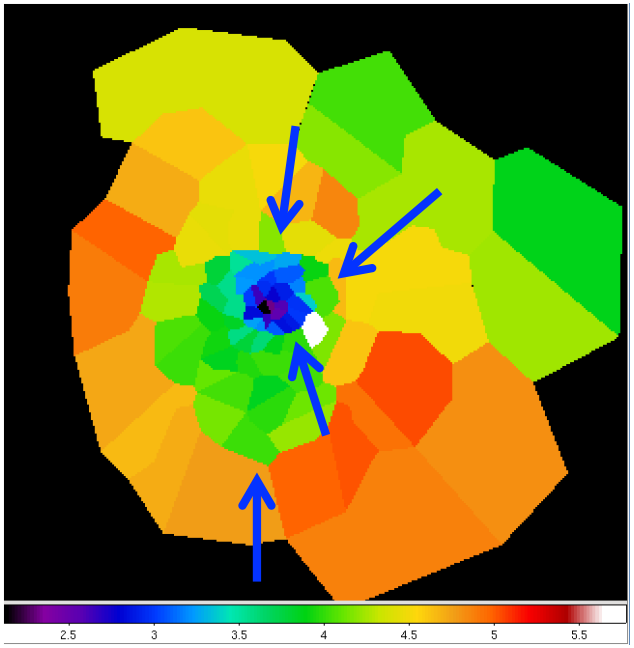

Iron Abundance

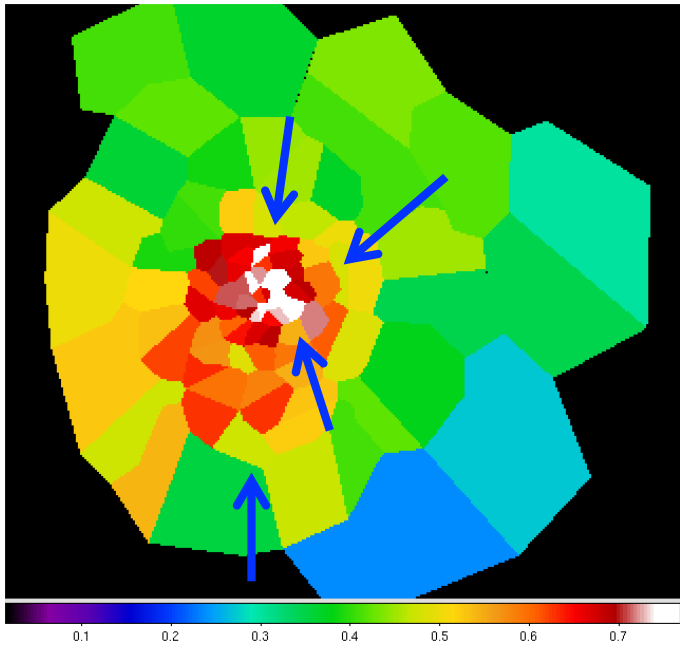

Entropy residuals

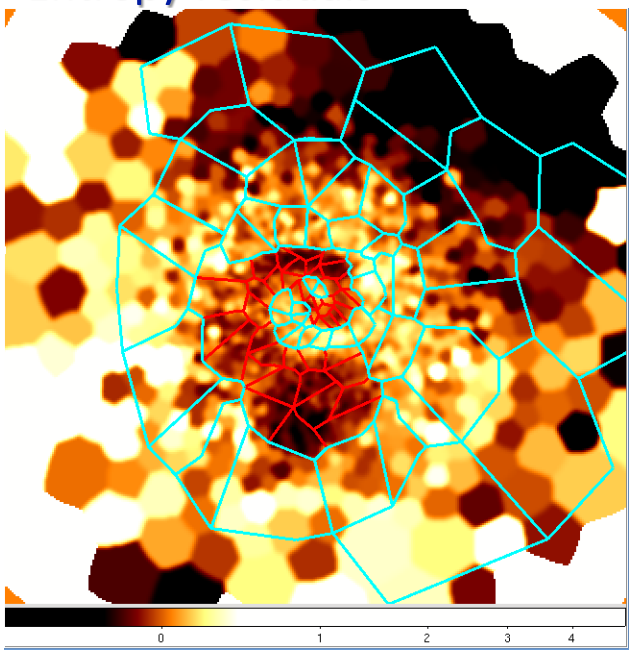

Ghizzardi, SD et al. 2013: Abell 496 XMM data

Temperature and Z_{Fe} profiles on the spiral

Ghizzardi, SD et al. 2013

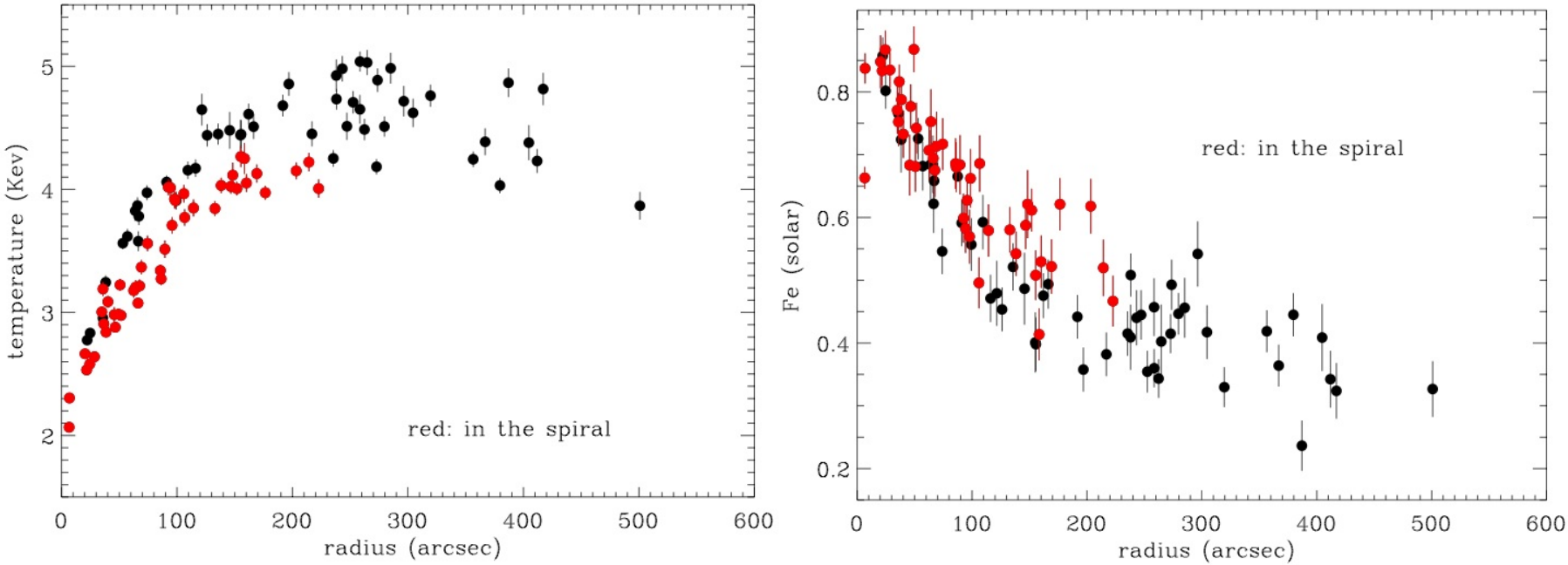

- **The temperature in the spiral regions is lower and the metallicity is higher.**
- The spread between points IN and OUT the spiral increases with the radius.

Temperature and Z_{Fe} profiles on the spiral

Ghizzardi, SD et al. 2013

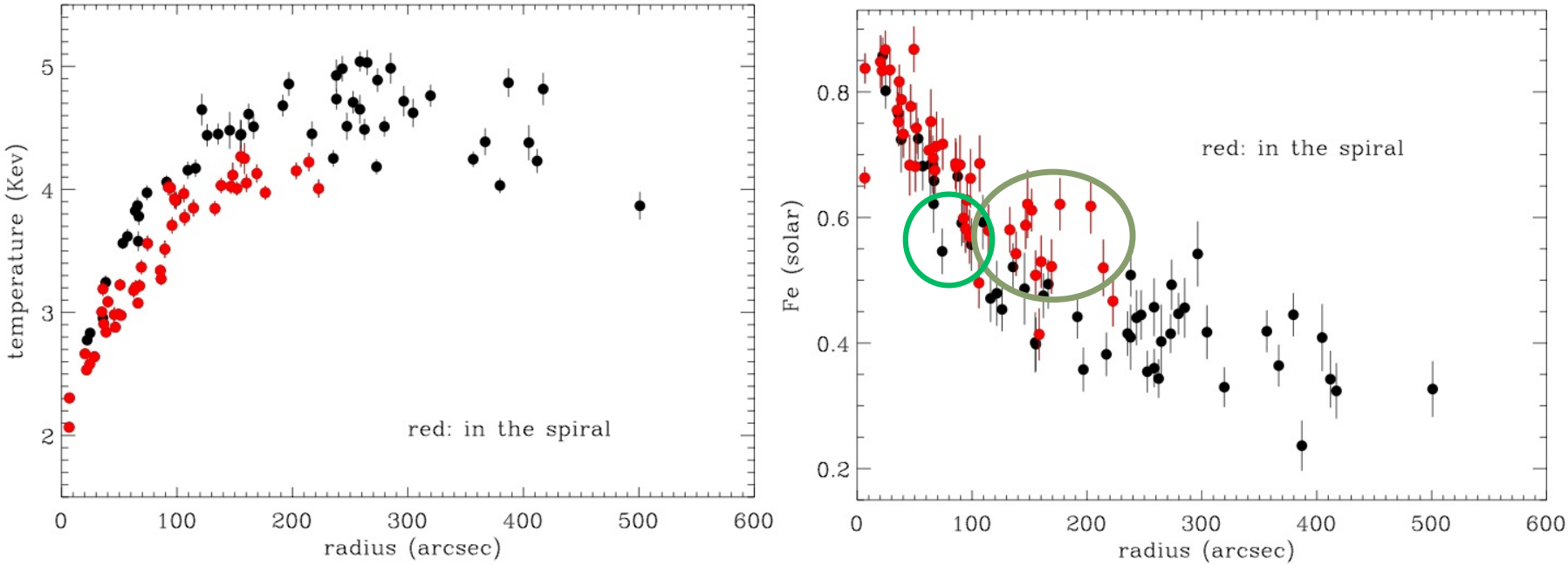

- **The temperature in the spiral regions is lower and the metallicity is higher.**
- The spread between points IN and OUT the spiral increases with the radius.
- The gas lying on the tail comes from a region located at ~60 kpc from the peak.
- **The central cool and metal rich gas is displaced outwards in a hotter and less abundant region of the cluster**

Summary of the Second Part

- By comparing the M_{Fe}^{exc} from WARPJ1415 with those of local CC systems we find that Fe abundance excess produced by the BCG was already in place at z=1.
- To reproduce the M_{Fe}^{exc} we require a SN Rate of 2.2-3.4 SNu
- We propose a scenario where the bulk of the Z_{Fe} peak build up occurred immediately after the BCG formation phase at high z.
- While for local CC clusters the Fe distribution is broader than the optical light distribution, in WARPJ1415 the two distributions are consistent indicating that the process responsible for broadening the Fe distribution in local systems has not yet started in this distant cluster.
- The Fe peak broadening time scale can be very long (larger than ~8 Gyr).

FUTURE WORK:

- **A systematic follow-up with CC clusters from the CLASH (Postman+12) survey in the intermediate redshift range ~ 0.2 - 0.6.**